Malaria molecular surveillance in the Peruvian Amazon with a novel highly multiplexed *Plasmodium falciparum* Ampliseq assay

Johanna Helena Kattenberg[a#], Carlos Fernandez-Miñope[b,c], Norbert J. van Dijk[a,1], Lidia Llacsahuanga Allcca[b], Pieter Guetens[a], Hugo O. Valdivia[d], Jean-Pierre Van geertruyden[c], Eduard Rovira-Vallbona[a], Pieter Monsieurs[a], Christopher Delgado-Ratto[b,c], Dionicia Gamboa[b,e], Anna Rosanas-Urgell[a]

[a]Institute of Tropical Medicine Antwerp, Biomedical Sciences Department, Antwerp, Belgium

[b]Instituto de Medicina Tropical "Alexander von Humboldt", Universidad Peruana Cayetano Heredia, Lima, Peru

[c]Global Health Institute, University of Antwerp, Antwerp, Belgium

[d]Department of Parasitology, U.S. Naval Medical Research Unit No 6 (NAMRU-6), Lima, Peru

[e]Departamento de Ciencias Celulares y Moleculares, Facultad de Ciencias y Filosofía, Universidad Peruana Cayetano Heredia, Lima, Peru

Running Head: Pf AmpliSeq assay for malaria molecular surveillance

address correspondence to: ekattenberg@itg.be and arosanas@itg.be

[1] Present address: N.J. van Dijk, Department of Medical Microbiology, Amsterdam University Medical Centers, Amsterdam, the Netherlands

[2] Present address: Barcelona Institute for Global Health, ISGlobal, Barcelona, Spain

Abstract

Molecular surveillance for malaria has great potential to support national malaria control programs (NMCPs). To bridge the gap between research and implementation, several applications (use cases) have been identified to align research, technology development, and public health efforts. For implementation at NMCPs, there is an urgent need for feasible and cost-effective tools.

We designed a new highly-multiplexed deep sequencing assay (Pf AmpliSeq), compatible with benchtop sequencers, allowing for high accuracy sequencing at higher coverage and lower cost than WGS, targeting genomic regions of interest. The novelty of the assay is in its high number of targets multiplexed in one easy workflow, combining population genetic markers with 13 near full-length resistance genes, applicable for many different use cases. We provide a first proof-of-principle for *hrp2* and *hrp3* deletion detection using amplicon sequencing. Initial sequence data processing can be performed automatically, and subsequent variant analysis requires minimal bioinformatic skills using any tabulated data analysis program.

The assay was validated with a retrospective sample collection (n = 254) from the Peruvian Amazon between 2003 and 2018. By combining phenotypic markers and a within-country 28-SNP-barcode, we were able to distinguish different lineages with multiple resistant (*dhfr/dhps/crt/mdr1*) haplotypes and *hrp2* and *hrp3* deletions, increasing in recent years. We found no evidence suggesting the emergence of ART-resistance in Peru. These findings indicate a parasite population under drug pressure, but susceptible to current antimalarials, and demonstrates the added value of a highly multiplexed molecular tool to inform malaria strategies and surveillance systems.

Importance

While the power of next generation sequencing technologies to inform and guide malaria control programs has become broadly recognized, integration of genomic data for operational incorporation into malaria surveillance remains a challenge in most malaria endemic countries.

The main obstacles include limited infrastructure and accessibility to high-throughput sequencing facilities and the need for local capacity to run in-country analysis of genomes at a large enough scale to be informative for surveillance. In addition, there is a lack of standardized laboratory protocols and automated analysis pipelines to generate reproducible and timely results useful for relevant stakeholders.

With our standardized laboratory and bioinformatic workflow, malaria genetic surveillance data can be readily generated by surveillance researchers and malaria control programs in endemic countries, increasing ownership and ensuring timely results for informed decision and policy-making.

Introduction

The Global Technical Strategy for Malaria 2016-2030 identified the use of high-quality surveillance data for decision-making as an essential pillar for malaria elimination (1). In view of current challenges to malaria control (*e.g.* spread of drug resistance, changing transmission intensity, risk of malaria importation in malaria-free areas, and RDT-failure), genetic epidemiology is increasingly recognized in its

potential to inform national malaria control programs (NMCPs). By aligning multiple scientific fields in support of NMCP priorities, 'use cases' were specified creating scenario's where genetic surveillance can be informative to decision-making (2, 3), and can be used to develop and implement new technologies.

Molecular markers associated with drug resistance are reliable predictors of treatment responses (2, 4, 5), can provide warning for emerging resistance, guide treatment policies (6), and even replace therapeutic efficacy studies in low malaria transmission areas (4, 5, 7, 8). The value of these markers was demonstrated in Southeast Asia where *P. falciparum* resistance against artemisinin (ART) was associated with mutations in the Kelch protein 13 (*K13*) (9-12), and resistance mutations in this same gene recently emerged in Africa (13).

In addition, monitoring population genetic markers can guide control and elimination strategies by identifying drug resistance gene flow, distinguishing imported from autochthonous cases and estimating the source of reintroduced cases in malaria-free areas (2, 14-16). Parasite genetics can identify underlying patterns of transmission and transmission intensity (17).

The gene products of *P. falciparum hrp2* and *hrp3* are detected by rapid diagnostic tests (RDTs), and gene deletions resulting in false-negative RDT results were first detected in Peru 10 years ago (18). Since then, there have been more reports from many areas (19-22)(23, 24), raising concerns for the viability of HRP2-based RDTs. The WHO recommends assessing prevalence of *hrp2* and *hrp3* mutants among malaria patients and to change case-management strategies when more than 5% of infections contain deletions (25).

Different genetic markers are required to address the forementioned challenges, and are most efficiently targeted in a single genomic tool (3, 26). Whole genome sequencing (WGS) can provide the highest information content per sample, however, implementing WGS for surveillance is constrained by the limited access to high-throughput sequencers and lack of technical and bioinformatic skills in endemic countries. As a result, sequencing is often performed through genomic consortia, delaying the turn-around-time from sample collection to genetic data, and limiting its usefulness to NMCPs. In addition, obtaining high-quality WGS data from low density infections and dried blood spots (DBS) remains challenging. Consequently, it is rare for genomic surveillance to be used beyond research (27-29).

Targeted Next Generation Sequencing (NGS) tools are emerging that combine numerous targets of interest into one workflow and more time and cost-efficient than WGS or traditional PCR-based approaches with amplicons detected by different techniques (10, 30-33). Laboratory protocols for NGS-assays are well-standardized, sequencing is feasible on benchtop sequencers and automated analysis pipelines are available (2, 6), for example the MaRS assay (34) that targets multiple drug resistance markers. While microsatellites have frequently been used for population genetic surveillance as they are not under evolutionary pressure, these markers are not easily translated to NGS due to the short repetitive nature of the variation. Instead, SNP barcodes can be successfully targeted by NGS (35-37), are informative for connectivity between populations (38, 39) and prediction of infection origin (40, 41). The SpotMalaria platform combining drug resistance markers with a SNP barcode was helpful in tracking the rapid spread of resistant parasites in the Greater Mekong Subregion (42).

99 Currently, there is no multifunctional tool suitable for more than two 'use cases'. The characterization of
100 *hrp2* and *hrp3* deletions still relies on PCR assays that classify deletions based on failure to amplify
101 targets (23). The few existing tools that combine population markers with drug resistance target short
102 regions around validated resistance SNPs, missing the potential to detect novel resistance associated
103 mutations. Furthermore, many SNP-panels were designed from genomes across the world and lack the
104 resolution to study subtle patterns on a smaller geographical scale. Therefore, we designed a targeted
105 NGS-assay (Pf AmpliSeq) that combines a specifically designed barcode for the target country, 13 full
106 length resistance associated genes, *hrp2* and *hrp3*, and a *ama1* microhaplotype region. The assay is
107 applicable to DBS and adaptable to different settings. The AmpliSeq technology (43) applies a multiplex
108 PCR to simultaneously amplify a high number of targets in a rapid procedure, and allows overlapping
109 amplicons to cover large genes.

110 We applied the Pf AmpliSeq assay to Peruvian samples for assay validation. *P. falciparum* in Peru makes
111 a good case-study, as malaria elimination is on the regional agenda (44), with countries first targeting *P.*
112 *falciparum* elimination due to its lower case load than *Plasmodium vivax*, but also in fear of emerging
113 ART-resistance. South America has been a hotspot for chloroquine (CQ) and sulphadoxine-
114 pyrimethamine (SP) resistance evolution (45). More recently, *K13*-mediated ART-resistance emerged in
115 Guyana (46, 47), and *K13*-independent delayed parasite clearance after ART-treatment was reported in
116 Suriname (46, 48, 49). *P. falciparum* elimination is also threatened by the increasing prevalence and
117 spread of *hrp2* and *hrp3* deletions (21, 23).

118 Peru reduced malaria case incidence by ≥40% in 2010 (Figure 1), and, after a resurgence in 2016, cases
119 have been decreasing in the past 5 years after introduction of focal screening and treatment (50). Past
120 high levels of CQ and SP-resistance (51-54) led to Peru becoming one of the first countries in the
121 Americas introducing artemisinin combination therapy (ACT) in 2001 (54-56). However, ACT efficacy and
122 drug-resistant markers have not been monitored in Peru since 2009. In 1998-2001 up to 20% of
123 infections in Peru were *hrp2* deleted, increasing to 53% *hrp2* deletions and 37% deletions of both genes
124 in 2012-2014 (18, 19). In this study, we demonstrate the added value of molecular surveillance in Peru
125 with different 'use cases' using our Pf AmpliSeq assay and explore the changes of the parasite
126 population in the past two decades.

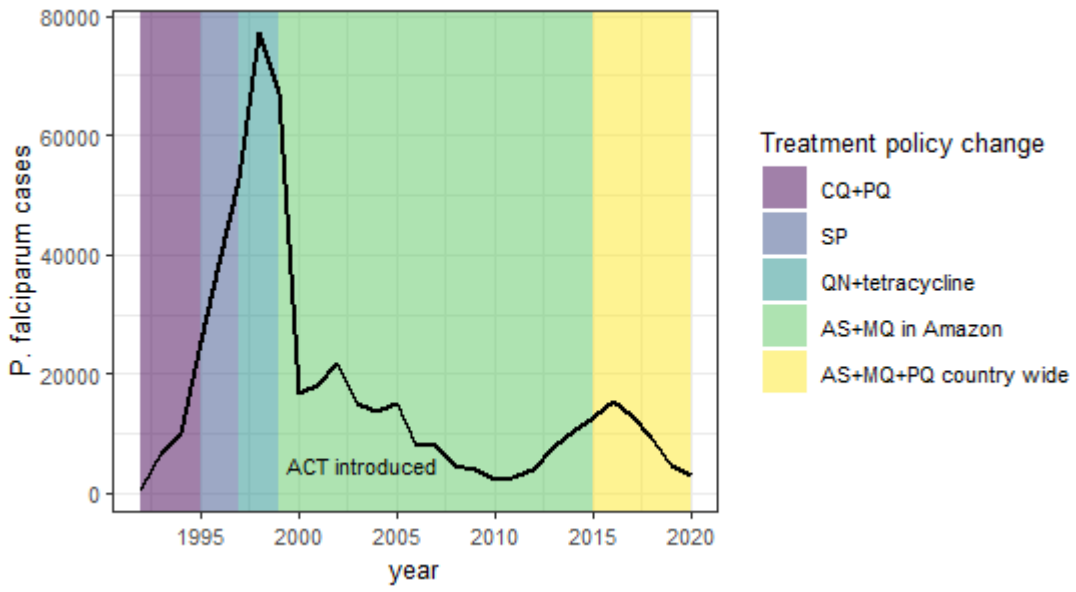

Figure 1 – Annual *P. falciparum* cases in Peru (black line) from 1992-2020, with first-line treatment policy changes (source of data: Centro Nacional de Epidemiología, Prevención y Control de Enfermedades (2020) Sistema de Atención de Solicitudes de Acceso a la Información Pública Vía internet del Ministerio de Salud. Available at: http://www.minsa.gob.pe/portada/transparencia/solicitud/). Artemisinin combination therapies were first introduced in the Amazon region in Peru in 2001, contributing to a dramatic decline in cases. Artesunate mefloquine with primaquine (AS + MQ +PQ) has always been the recommended first-line treatment in the Amazon region (51) with continued high efficacy (57), and AS+SP was used on the North Coast. In 2015, AS+MQ+PQ became the recommended first-line treatment in the whole country (58). Peru reduced malaria case incidence by ≥40% by 2010 using passive case detection (PCD), diagnosis with light microscopy and treatment with AS+MQ as main components of the control program (59). In 2015, with the realization that PCD missed asymptomatic infections (60), focal screening and treatment was introduced, resulting in a further reduction of malaria incidence (50). CQ + PQ = chloroquine + primaquine; SP = sulfadoxine-pyrimethamine; QN = quinine.

Results

Pf AmpliSeq design and performance

A panel of 13 *P. falciparum* drug resistant associated genes (Table 1) and corresponding variants of interest, *i.e.* (putative) resistance associated mutations (Supplementary file 1), were included in the assay design. The selected genes included validated mutations (4, 7) or variants relevant for Peru, *i.e.* previously reported or associated with historically- and currently-used drugs. Additional targets were: *hrp2* and *hrp3* genes, the apical membrane antigen 1 (*ama1*), conserved *Plasmodium* membrane protein (*cpmp)* (61) and microsatellites (MS) *poly-alpha, ARAII, TA81* and *PfPK2* (62). We designed a barcode of 28 SNPs with in-country resolution in Peru (Supplementary file 3). The final assay included >85% of desired regions in 233 amplicons (Supplementary file 2) with varying amplicon length (55-323 bp). The *cpmp* region and a small section of the *crt* gene failed in the primer design, including *crt* variant I218F.

We validated the assay with *P. falciparum* cases (n=312, Figure 2) from multiple previous studies in Peru, laboratory strains (n=5), and previously genotyped isolates (n=6) as controls. A high number of reads was generated in the assay (mean 217,037 ± 490,478 paired reads/sample after trimming low quality reads) with a median of 99.6% [range 3.9-99.9%] of trimmed reads aligning to the Pf3D7 genome.

Targets regions were covered with a mean 1,336±3,627 paired reads (range 20-43,795). To improve nucleotide diversity in the run (30% GC content), we tested a 20% spike-in of PhiX-library, however, this is not recommended as it did not result in a more high-quality reads (9.7%±10.6 poor quality reads were trimmed without spike-in *vs.* 10.3%±7.3 with spike-in), and reduced total read number.

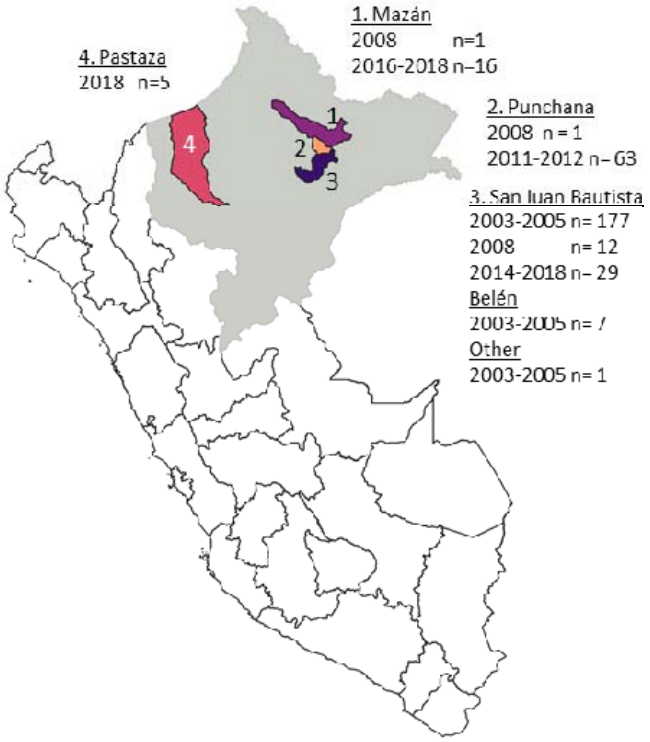

Figure 2 – Map of study sites of retrospective sample collection from the Peruvian Amazon region Loreto (grey). The majority of samples were collected in Maynas Province (areas 1, 2, and 3): samples collected in/near the San Juan Bautista district (area 3), which covers part of the urban area of Loreto's capital Iquitos and peri-urban communities south of Iquitos (n=226), and samples from the Mazán district (area 1; n =17) and Punchana district (area 2; n =64) with remote communities living near forest rivers such as the Amazon River and Napo River, North of Iquitos. A final collection of samples from 2018 was available from the Northern Amazon region in Datem del Marañón Province, Pastaza District (area 4, n=5). *P. falciparum* positive samples from previous studies were selected based on geographical representation and parasite density (≥100 p/µl by PCR; geometric mean density 4300±3.1 p/µl).

Depth of coverage

Median amplicon depth of coverage of aligned high quality reads past filter (DP) was 82.9 [IQR 42.9-116.1] (Figure S1). Fifteen (6.4%) amplicons had poor DP (<10; Table S1), while six (2.6%) had high DP (>150; Table S2). Among those, four *hrp2* and *hrp3*-amplicons had lower DP in the study samples, but not in controls, due to high prevalence of deletions in these genes. Lower DP in other amplicons is likely due to sequence variation in primer binding sites, resulting in poor amplification and high amount of missing data in these regions, *e.g.* A220S in *crt*. In contrast, two *hrp2*-amplicons had much higher depth than average, possibly due to cross-alignment between *hrp2* and *hrp3* repetitive regions. In 23/233 amplicons no variants (*i.e.* only reference alleles) were detected despite good amplification and sequencing (Table S3), and these amplicons were in conserved regions of drug resistance genes.

179 **Uninfected controls**

180 Primer specificity was tested with four uninfected human blood samples (negative controls), and none
181 of these resulted in genotypes in the assay target region. We did observe background sequences, with a
182 very low number of reads corresponding to multiple unspecific hits to Plasmodium and human
183 sequences; all of them outside the assay target regions and below the filtering threshold.

184 Eight stored previous library preparations (incl. control samples and one human negative) were included
185 to test replicability, but this resulted in a contamination in the human negative. In the initial run this
186 control was not contaminated, and none of the new library preparations were contaminated with these
187 specific genotypes.

188 **Parasite density limit and selective whole genome amplification**

189 DP decreased while missingness increased with decreasing parasite density in a dilution of 3D7 (6000 to
190 6 parasites/µl (p/µl)) at a DNA concentration mimicking dried blood spots (DBS). At the lowest density (6
191 p/µl), DP was only 10, and 60% of loci were missing. Selective whole genome amplification (sWGA) prior
192 to library preparation improved the number of high quality reads at parasite densities below 60 p/µl
193 (Figure S2); with 10-fold more reads at 60 p/µl to 90-fold at 6 p/µl.

194 **Error-rate and reproducibility**

195 Sequencing accuracy was higher in biallelic SNPs (mean error-rate 0.008%±0.004) compared to indels
196 (0.02%±0.005) (Table S4). At parasite densities >6 p/µl, sWGA is not recommended, as error-rates were
197 higher with sWGA (0.13% ± 0.06) than without (0.05% ± 0.01), with little gain in coverage.

198 The reproducibility of the assay was tested, with a median difference of 4 SNPs (0.6% of SNP loci;
199 0.007% of 57445bp targeted in the assay) between sample and control replicates observed. With indels
200 and multiallelic variants, a median difference of 50 alleles (2.8% of loci; 0.09% of 57445bp) was
201 observed.

202 In comparison to previous results with laboratory strains and control samples, 97.6% of genotypes were
203 accurate (Table S5). In the control samples, 7.9% additional heterozygous genotypes were detected by
204 AmpliSeq, which might have been previously undetected minor clones due to lower sequencing depth in
205 the SpotMalaria pipeline and WGS data.

206 **Complexity of Infection**

207 Minority clones could be detected in the Pf AmpliSeq assay up to a 80:20 of 3D7:Dd2 mixture with
208 43.8% (28/64) Dd2-loci detected (Table S6). Below 95:5 few Dd2-genotypes were detected.

209 The complexity of infection (COI) estimates the number of genetically distinct clones in an infection,
210 which can be used as a proxy for transmission intensity (16, 63). We applied different methods to
211 determine COI from NGS, but results varied considerably by method (Table S7). Therefore, we
212 determined the most frequent value (mode) of COI, which showed an increasing proportion of multiple
213 clone infections in Peru over time (13.8% in 2003-2005; 28.8% in 2008-2012; 33.3% in 2014-2018; X^2
214 p=0.0005) (Figure S3).

215 **Use case *hrp2* and *hrp3* gene deletions**

216 Compared to prior PCR-classification, all samples (10/10) were correctly classified for 'RDT-failure'
217 (deletion of both genes) *vs.* 'RDT-detectable' (presence of one or both genes) using the read depth of
218 *hrp2* and *hrp3* amplicons. For 6/10 samples, classification was correct for both genes, but in 4 four
219 samples the *hrp2*-classification was inconclusive (Table S8), due to discrepancy in classification between
220 amplicons.

221 With the Pf AmpliSeq assay, 94.9% (241/254) of study samples could be classified as 'RDT-failure' or
222 'RDT-detectable'. The proportion of individuals with 'RDT-failure' increased from 17.7% in 2003-2005 to
223 42.6% in 2008-2012 and 73.3% in 2014-2018 (X^2, p>0.001). While *hrp3* presence *vs.* absence could be
224 determined for most samples (96.5%), 26.8% of *hrp3*+ samples were inconclusive for *hrp2* (Figure S9),
225 but since they were not *hrp3* deleted, were classified as 'RDT-detectable'.

226 **Barcode performance**

227 All 28 barcode SNPs were detected in the assay (Table S9), although one (Pf3D7_12_1127001) was
228 genotyped as an indel. In the study samples, population minor allele frequencies (MAF) of the barcode
229 SNPs ranged between 0.35-0.50 at 9 loci, between 0.1-0.34 at 12 loci and <0.1 at 7 loci. We did not
230 observe the minor allele of one of the barcode SNPs (Pf3D7_05_921893) in the study samples, although
231 it was detected in laboratory strains (n=5), and 5/6 control samples.

232 **Use case transmission intensity: Genetic diversity & differentiation**

233 Principal component analysis (PCA) showed sample clustering by year rather than collection site (Figure
234 S4), therefore the samples were divided in three time periods for subsequent analyses: 1) early time
235 period (2003-2005), 2) intermediate time period (2008-2012), and 3) most recent period (2014-2018)
236 where little variability was observed.

237 Genetic diversity (expected heterozygosity, *He*) of the parasite population, was lower in 2008-2012
238 (p=0.003) and 2014-2018 (p=0.00004) than in 2003-2005 (Figure 3A). Total population size was small, as
239 the observed heterozygosity (*Hobs*) was lower than *He* (p<0.005), indicating that genetic diversity was
240 lower than expected from a population in Hardy-Weinberg equilibrium. The parasites in 2008-2012 and
241 2014-2018 showed great genetic differentiation (F_{ST}>0.25) compared to parasites in 2003-2005 (Figure
242 3B). The parasite population changed considerably since 2008, with a less diverse and smaller
243 population.

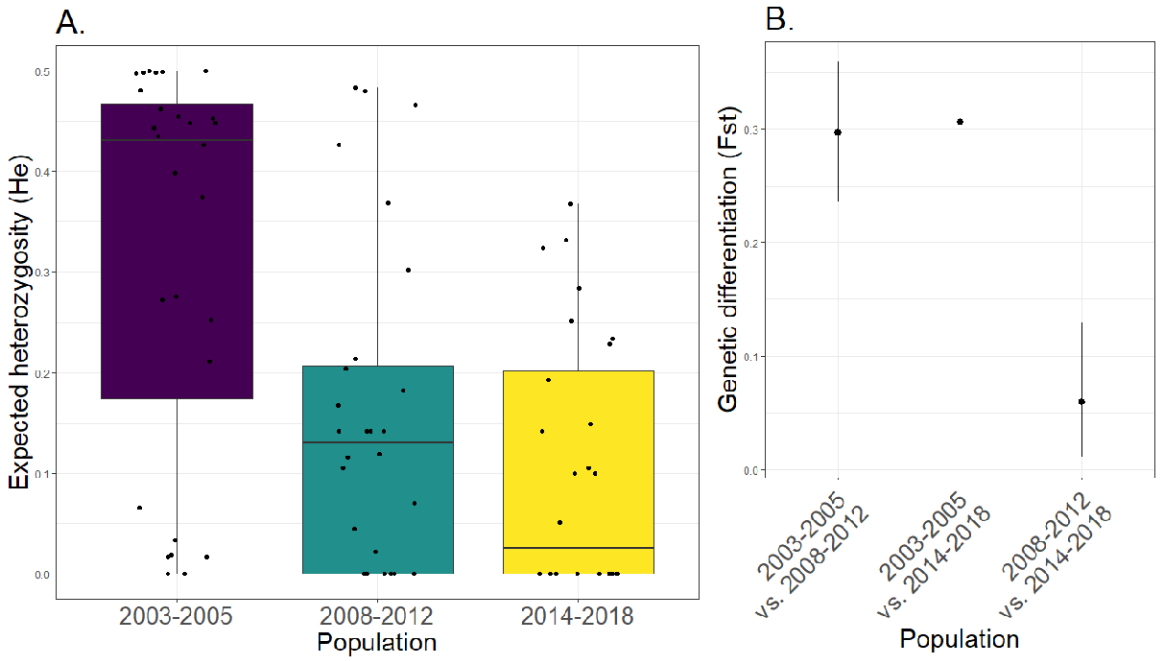

Figure 3 - Population genetic statistics. A) Genetic diversity (expected heterozygosity, *He*) for each barcode locus (black dots) grouped by time-period. Boxplots show a decrease in the median [interquartile range] of *He* after the first time period (2003-2005). Since differences in He might be due to unequal sampling in districts through time, we assessed He within San Juan Bautista district that was sampled at all three time-periods. This confirmed decreasing diversity over time, with a pronounced decrease in He in 2014-2018 ($p > 0.001$, Figure S5 and table S10). **B)** Genetic differentiation between the three populations measured as F_{ST} (Weir & Cockerham, 1984) using the R package diveRsity. Number of individuals for each population: $n_{2003\text{-}2005} = 118$; $n_{2008\text{-}2012} = 65$; $n_{2014\text{-}2018} = 38$. In Figure S5 *He* by time and district is plotted and in Figure S6 the differentiation measures $G`_{ST}$ (Hedrick, 2005) and Jost's D (Jost 2008) are plotted.

Use case connectivity of parasite populations: Barcode multilocus lineages and population structure

We identified 36 multilocus (ML) lineages with distinct barcodes in the study population over time (Figure 4) and districts (Table 2). The distinct lineages clarify the significant linkage disequilibrium (LD) in the barcode in all time periods and districts (Table S11). In 2003-2005 we observed 23 lineages, and only 11 in 2008-2012, matching the decrease in *He*.

Lineage no. 155 became predominant after 2008, with many related lineages (Figure S7), explaining the small population size and increasing number of barcode alleles that become fixed (2 in 2003-2005; 8 in 2008-2012; 14 in 2014-2018; Table S12). The predominant lineage was in in co-existence with others within district and period. The ML-lineages in later periods (2008-2018) changed considerably since 2003-2005 paralleling observed F_{ST}.

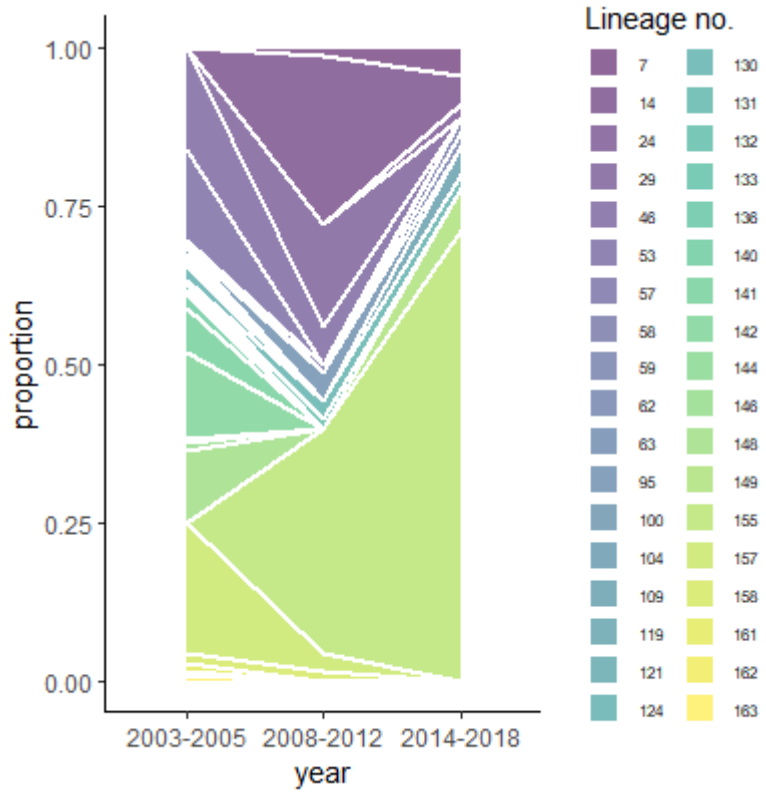

Figure 4 - Dynamics of 28-SNP barcode multilocus lineages. Area plot showing the proportions of each ML-lineage detected in the three different time periods in study samples (n=254) from Peru. ML-lineages were identified, clustered using genetic distance between barcodes with the poppr package in R, and given an identifying number. ML-lineages differed by multiple SNPs (≥4 SNPs), enabling lineage classification even when barcodes had some missing or heterozygous genotypes. Lineages are characterized by unique barcodes and resistance genotypes and listed in table 2.

With discriminant analysis of principal components (DAPC), the resolution increased to all biallelic variants (n_{loci}=772), and we determined the underlying causes of the population differentiation (Figure 5). The highest contributing alleles along the first axis (2003-2005 *vs.* 2008-2018) were drug-resistance mutations *dhfr* C50R and N51I, *mdr1* D1246Y, and *dhps* K540E (Table S13). Contributors to the differentiation along the second axis (2014-2018 and Pastaza) were seven barcode SNPs and *dhfr*, *mdr1*, *coronin* and *ubp1*-variants.

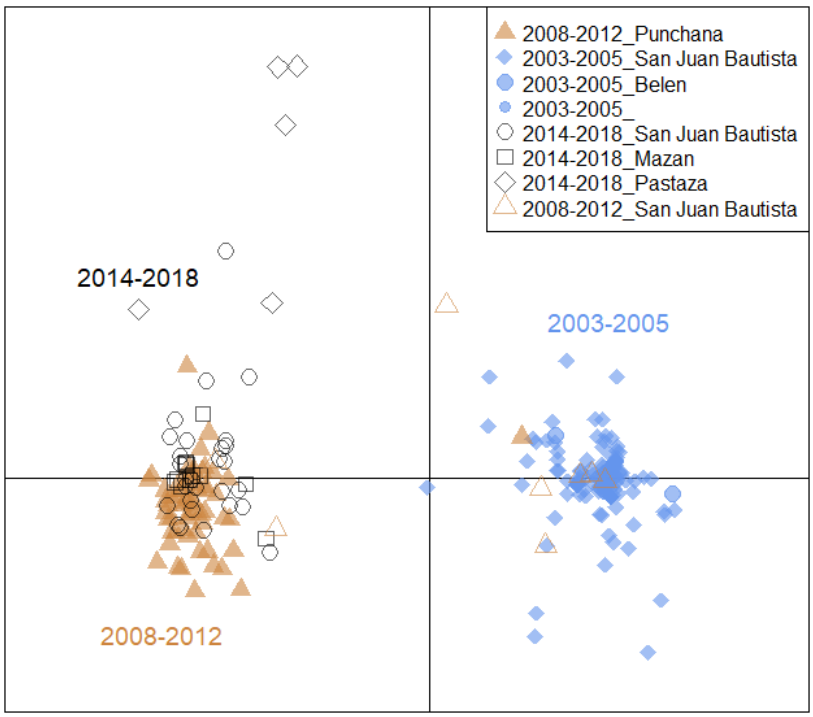

Figure 5 - Discriminant analysis of principal components (DAPC). Scatter plot of discriminant analysis (DA) eigenvalues 1 and 2 using all biallelic SNPs in the core targeted region (excl. amplicons targeting repetitive regions and non-nuclear targets), showing a differentiation between Peruvian *P. falciparum* samples collected before 2008 and those afterwards (x-axis, PC1), and a subsequent separation along the y-axis (PC2) from 2014 to more recent years and along geographic distance. SNPs contributing most to the DAPC are listed in Table S13. DAPC was performed with 40 principal components and 7 discriminants as determined through cross-validation. The increased resolution in the DAPC allowed the detection of greater genetic variation in isolates from 2014-2018 (black shapes), compared to lineage analysis.

Use case drug resistance: Artemisinin resistance-associated genes

The full-length *K13* gene was amplified with 12 overlapping amplicons. We detected several ART-resistance validated SNPs in control samples, but did not observe these SNPs (F446I, N458Y, M476I, Y493H, R539T, I543T, P553L, R561H, P574L and C580Y) in the study samples. We observed several low frequency mutations in the K13-propellor region (V445A, I448K, G449C, V581I, premature stop codon at 613; Table 3), always in mixed infections. Outside the propeller region, the K189T mutation was observed at a high frequency (63%-84%).

Forty-four amplicons covered the *ubp1* gene (91.8% of the gene), including all variants of interest. Previously reported variants (incl. R3138H) were not detected, but we observed a change in the predominant *ubp1*-haplotype. In 2003-2005, a haplotype with Q107L, commonly with K1193T, was most frequently observed (42.6%; Table 3). In later years, R1133S-haplotypes (often linked with E1011K) replaced the Q107L-haplotypes.

Eleven amplicons amplified full-length *coronin* gene. We identified two novel mutations V62M and V424I, and none of the *in vitro* associated variants. V62M was seen at 20.6% in 2003-2005, but decreased over time (Table 3). V424I increased from 55.4% in 2003-2005 to 80.9% in 2014-2018 (Table

301 3). While V62M is located in the WD-40 beta-propeller domain (containing validated mutations G50E,
302 R100K and E107V), V424I is located just outside this region and is not expected to contribute to ACT
303 resistance.

304 **Use case drug resistance: CQ and ACT partner drug resistance associated genes**
305 The SP-resistance associated genes were each targeted with 9 amplicons, covering 100% of *dfhr* and
306 87% of *dhps*, incl. all variants of interest. In 2003-2005 we observed predominantly single (69.5%) and
307 double (22.7%) *dhfr* mutants, and wildtype (*wt*) *dhps* (≥56.7%; Table 3). Although SP-use was
308 discontinued in 1999, after 2008, SP-resistance increased with high frequency of triple mutants in *dhfr*
309 and *dhps*. Consistent with previous reports (45, 64), we did not detect *dhfr* C59R in Peru. Therefore, the
310 'sextuple' mutant here is different from the African sextuple mutant, with C59R instead of C50R, but
311 similar super resistant phenotype (65).

312 Sixteen amplicons covered the *crt* gene (91.1%), missing one variant of interest (I218F) associated with
313 PPQ resistance. CQ resistance (CQR) *crt* haplotypes, CVMNT (CQR) and SVMNT (highly CQR), increased
314 over time (Table 3) with 100% SVMNT in 2014-2018. The mutation I356V, whose contribution to CQR is
315 unclear, was frequent (>93%) in all time periods.

316 Eighteen amplicons covered the *mdr1* gene (87%), targeting all variants of interest associated with CQ
317 and MQ-resistance (7). While the *mdr1* haplotypes NDFCDD and NGFSDD were predominant in 2003-
318 2005, in later years it was mainly the NDFCDY haplotype (Table 3). There are conflicting results on the
319 association of NDFCDY with susceptibility to MQ, AS and CQ (64, 66). The *mdr1* D144G SNP has so far
320 only been reported in Peru (annotated as D142G in (64)) and is decreasing in recent years.

321 Copy number variations (CNVs) in *mdr1* and *plasmepsin II* associated respectively with PPQ (67) and MQ
322 (68) resistance were not previously observed in Peru (69). We confirmed single copies of both genes by
323 qPCR in a subset of 78 samples (Figure S8). While both genes were sequenced in our assay, the lack of
324 increased copy numbers resulted in insufficient data to validate CNV detection by Pf AmpliSeq.

325 We did not detect many variants of interest in the other targeted genes, with 10.6% of the S160N
326 mutant in 2003-2005 in the *ap2-mu* gene (9 amplicons covering 99.1% of the gene), which decreased in
327 later periods (1.5% and 2.2%). No variants of interest were observed in *pfmrp1* (95.1% covered),
328 *pfexonuclease* (98.6% covered), *cytochrome B* (100% covered) and *23S rRNA* gene (100% covered).

329 **Use case drug resistance gene flow: drug resistance and parasite lineage evolution**
330 Between 2003 and 2005, we observed lineages with predominantly single and double *dhfr* mutants, *wt*
331 *dhps*, CVMNT and SVMNT *crt*-haplotypes, multiple *mdr1*-haplotypes and presence of *hrp2* and *hrp3*
332 deletions (Table 2). From 2008, the majority of parasite lineages harbored sextuple *dhfr/dhps* mutants,
333 *crt* SVMNT, *mdr1* NDFCDY, and *hrp2* and/or *hrp3*-deletions. Parasites with this *dhps/dhfr/crt/mdr1*
334 resistance haplotype and both *hrp2* and *hrp3* deleted were first reported in few cases from Peru in 2006
335 (64) and called the B_{V1}-lineage. Here, we observed many parasites with the same 'B_{V1}-type' resistance
336 haplotype, although not always with *hrp2* and *hrp3*-deletions. With the greater resolution in the Pf
337 AmpliSeq assay, we observed many related lineages with this resistant haplotype that differ in the
338 barcode genotype, presence of *hrp2* and *hrp3*-deletions, and *coronin* SNPs (Table 2). This indicates gene
339 exchange between lineages contrasting the idea of isolated clonal lineages in Peru.

340 The B_{V1}-type lineages are closest related to earlier lineages 158, 141 and 63 in our study samples (Figure
341 S7), but the triple *dhfr* mutants are not accompanied by the secondary mutations (I164L and the
342 "Bolivian Repeat" (BR), a silent 5 amino acid insertion before codon 30), indicating that they did not
343 emerge from the double *dhfr* lineages circulating in earlier years. In conclusion, the combination of
344 different markers in the Pf AmpliSeq assay allowed the identification of multiple recombining *P.*
345 *falciparum* lineages in Peru that share increasing SP and CQ resistance, as well as RDT failure, in more
346 recent years.

347 **Discussion**

348 We designed a new highly-multiplexed sequencing assay (Pf AmpliSeq) targeting 13 antimalarial
349 resistance genes, combined with a country-specific 28-SNP barcode for population genetic analysis in
350 Peru and *hrp2* and *hrp3* genes to detect deletions that can cause false-negative RDT results. The novelty
351 and strength of this assay is in the many different types of markers multiplexed in one easy workflow,
352 making it suitable for many surveillance 'use cases'. Compared to other amplicon sequencing assays (30,
353 34, 70) and genetic surveillance platforms (71), the Pf AmpliSeq includes the highest number of drug
354 resistance associated genes, combined with an in-country SNP-barcode, as well as diagnostics resistance
355 markers.

356 This assay performs well on DBS samples with parasite densities ≥60 p/µl, and allows for high accuracy
357 sequencing at higher depth of coverage (100-1000 fold *vs*. 50-100 fold) and lower cost (Table S14) than
358 WGS. At densities <60 p/µl, sWGA prior to the Pf AmpliSeq assay increases the number of reads, but also
359 the error rate and cost. Initial raw data processing can be performed automatically using software of the
360 sequencer, with no need for linux-based pipelines as we have used (giving us more flexibility and insight
361 during the validation). Subsequent variant analysis can be performed on a regular computer with
362 minimal bioinformatic skills using any software that can analyze tabulated data.

363 While the assay was capable at detecting ART-resistance validated SNPs in *K13,* only non-validated SNPs
364 were detected at low frequency in the Peruvian samples used for assay validation. Without presence of
365 validated markers in *K13*, there is no evidence suggesting the emergence of ART resistance in Peru in
366 recent years (2003-2018). Mutations in other genes in the endocytosis pathway have been associated
367 with decreased sensitivity to ART in *in vitro* studies and changes in *ubp1*-haplotypes paralleled the
368 emergence of *K13* markers in Thailand (72-81). However, the observed *ubp1* and *coronin* mutations here
369 are uncharacterized. Genetic variants in KlC7, Eps15, Formin2 associated with *in vitro* ART resistance
370 (74-76, 78, 82) were not reported yet when the assay design was being completed. These genes will be
371 included in future versions of the assay.

372 This is the first proof-of-principle of an NGS-amplicon assay targeting *hrp2* and *hrp3*-deletions, detecting
373 56.3% samples with both *hrp2* and *hrp3* deleted. This might be an underestimation, since infections
374 containing mixed strains with and without deletions might be classified as 'RDT-detectable'. It was
375 difficult to classify *hrp2* for 22% of samples, due to conflicting results between *hrp2* amplicons. The
376 difference in read depth with different *hrp2* amplicons suggests that potentially only a part of the gene
377 is deleted, with (part of) the first exon still present. Better characterization of the genomic structure of

378 *hrp2*-deletions could improve amplicon design. In addition, copy number calling tools could be explored
379 for more systematic classification of *hrp2* and *hrp3*-deletions.

380 With the combination of phenotypic markers and the 28-SNP-barcode in the Pf AmpliSeq assay, we were
381 able to detect changing allele frequencies in resistance associated genes, but also to identify temporal
382 genetic differentiation in the parasite population, alongside a decrease in genetic diversity. The barcode
383 served to distinguish different lineages in multiple resistant (*dhfr/dhps/crt/mdr1*) haplotypes circulating
384 in recent years, and enabled the investigation of drug resistance evolution.

385 SP- and CQ-resistance in South America was reportedly spread from a single origin in the lower Amazon
386 (45), with five distinct clonal lineages circulating in Peru before 2006 (19, 64, 83), followed by frequent
387 outcrossing and lineage evolution (83). With the Pf AmpliSeq, we observe the same SP/CQ-resistant
388 lineages and their evolution over time, with increased resolution and additional variants detected in
389 other genes.

390 The BV_1-type lineages that increasingly dominate the Peruvian parasite population after 2008, are highly
391 SP/CQ-resistant, and can frequently escape HRP2-based RDTs. The Pf AmpliSeq assay could characterize
392 outbreaks, such as the BV_1-outbreaks in Tumbes (84) and Cusco (85). What pressure selected the BV_1-
393 type lineages is unclear, as there is no clear evidence of ART-MQ resistance (absence of *K13*-variants and
394 *mdr1* CNV) and HRP2-based RDTs are not commonly used in Peru. The high level of CQR (in *crt* and
395 *mdr1)* could be the result of CQ-treatment of co-endemic *P. vivax* cases. Co-infections are frequent (86),
396 and can occur with low density *P. falciparum*, and frequently misdiagnosed and treated as *P. vivax*
397 mono-infection (83). When the BV_1-type lineages first appear (2011), we observed strong population
398 differentiation and loss of secondary *dhfr* mutations, which supports the suggestions from others that
399 this lineage was introduced from other parts of the Amazon (84, 87), possibly Colombia (20, 21) or
400 Suriname (49). Analysis of isolates from neighboring countries could shed light on the evolution and
401 spread of resistance and *hrp2* and *hrp3* deletions in the region. Predicting the origin of imported
402 infections based on SNPs is possible (40, 41, 88), however, samples from neighboring countries were not
403 available to investigate the spatial dynamics within this study. Existing public WGS datasets lack isolates
404 from sufficient countries in South America for a comprehensive analysis.

405 Ideally, to update genomic regions of interest, periodic WGS of a subset of samples should be performed
406 to investigate the emergence of mutations not targeted by the Pf AmpliSeq assay. Newly identified
407 regions could be added to the design. Similarly, we can exchange the SNP-barcode for application in
408 different countries, resulting in a modular design adaptable to the needs of a particular setting. The
409 assay in its current form is limited to South America. However, we are validating Pf AmpliSeq assays for
410 South East Asia and Sub-Saharan Africa, including also other ART-resistance genes, and *P. vivax* Ampliseq
411 assays.

412 Conflicting COI results were obtained due to differences between methods. In addition, the variant
413 calling tool used here assumes a diploid genotype with balanced within-sample allele frequency, which
414 is frequently not the case in malaria complex infections. Alternative haplotype-based analysis
415 approaches are available (*e.g.* SeekDeep (89), HaplotypR (61), and DADA2 (90)) that might have a
416 greater capability at unraveling complex infections, and more suitable for relatedness analysis (*e.g.*

417 identity-by-descent (91)). These methods could work with the existing design, or by adding
418 microhaplotypes (70). However, they are less easy to use for drug resistant markers and overlapping
419 amplicons.

420 As half of the barcode SNPs became fixed in the most recent years, the usefulness of the barcode in
421 future years might be limited. This likely reflects a true decrease in diversity as the sample size was
422 sufficient, and there are closely related clonal lineages. The sample size in this study was comparable to
423 earlier reports from Peru (*e.g.* 220 samples in 1999 (83), 104 samples from 1999 and 62 from 2006-2007
424 (64)), but represents a limited proportion of the Peruvian *P. falciparum* population. A more systematic
425 sampling approach of dried blood spots at many more sites within the country would be ideal for
426 routine genetic surveillance.

427 **Concluding remarks**

428 This study described a *P. falciparum* population in Peru with increasing accumulation of drug and
429 diagnostic resistance and spread of these lineages can be a serious threat to *P. falciparum* elimination
430 throughout the Amazon region. This study highlights the importance of systematic resistance monitoring
431 in the country, which is currently lacking, and offers a surveillance tool for multiple genetic 'use cases'.
432 Implementation will require a structured approach that will most importantly not unnecessarily burden
433 existing health systems and is sustainable for the long term. A molecular surveillance network (GENMAL)
434 has been established to stimulate wide-scale implementation and standardization of markers for
435 surveillance. This network will be a platform for coordination of research in Peru, data sharing and
436 efficient translation of results into policy-advice and practical guidelines for malaria elimination in Peru.
437 The type of multiplex assay as presented here could be more broadly applicable for the wider Amazon
438 area and South America to fill the void of genetic data from this region.

439 Materials and methods

440 **Study sites, samples and controls**

441 *P. falciparum* positive samples (n=312) from previous studies were selected based on geographical
442 representation (Figure 2) and parasite density (≥100 p/µl by PCR). Samples from 2003-2017 (n=269)
443 were from studies led by Universidad Peruana Cayetano Heredia (UPCH) ((18, 92) and ongoing), and the
444 U.S. Naval Medical Research Unit 6 (NAMRU-6) (n=63). Samples from 2018 (n=5) were the only *P.*
445 *falciparum* positive samples from a Zero Malaria Programme collection in Loreto in collaboration with
446 UPCH.

447 DNA was extracted from DBS using the E.Z.N.A Blood DNA Mini Kit (Omega Bio-tek, Georgia, USA)
448 following instructions. Per sample, two pieces of ~0.5 cm^2 were cut out and 100µL DNA was eluted. *P.*
449 *falciparum* parasitaemia was qPCR quantified (93).

450 The studies were approved by local ethical review boards. Protocols were registered in the
451 Decentralized System of Information and Follow-up to Research (SIDISI) (numbers: 52707, 61703,
452 101645, 66235, 102725), and one clinical trial registered at clinicaltrials.gov (NCT00373607). The
453 NAMRU-6 study was approved by its Institutional Review Board in compliance with all applicable federal
454 regulations governing the protection of human subjects (protocol NMRCD.2007.0004). Individuals were

455 included in this study only if signed informed consent included a future-use clause, and secondary-use
456 was approved through the Institutional Review Board of the Institute of Tropical Medicine Antwerp
457 (reference 1417/20).

458 For the final analysis we selected 254/312 (81%) samples with good quality data (<50% missing
459 genotype calls, mean coverage >15) and retaining only one library of replicates (with lowest
460 missingness). With a sample size of 96 samples a MAF of 0.01 with 0.02 (2%) precision could be
461 detected, and with 381 samples MAF=0.01 with (1%) precision
462 (https://epitools.ausvet.com.au/oneproportion).

463 Laboratory isolates and uninfected human blood were included as controls (Table S15). Control samples
464 (n=6) with known variants from a previous study in Vietnam (94) genotyped with the SpotMalaria
465 pipeline and WGS were also included. DNA of controls (100µL) was extracted using QIAamp DNA Mini
466 Kit (Qiagen) following instructions. sWGA was performed as previously described (95). Genotypes of the
467 laboratory strains were from (69, 96-98).

468 **SNP-barcode design**

469 A barcode of 28 biallelic SNPs was designed (Supplementary file 3). Briefly, MalariaGEN *Plasmodium*
470 *falciparum* Community Project data (99) was used to select SNPs (0.35≤MAF≤0.5) contributing to
471 between-country differentiation using DAPC (100). Two SNPs per chromosome were selected with
472 priority for synonymous SNPs with low pairwise-LD.

473 **Pf AmpliSeq workflow and sequencing**

474 Library preparation was performed using AmpliSeq Library PLUS for Illumina kit (Illumina), AmpliSeq
475 Custom Panels (Supplementary file 2) and AmpliSeq CD Indexes (Illumina) as per the manufacturer's
476 instructions. DNA concentration for controls and 25 samples was determined using Qubit v3 High
477 sensitivity DNA kit (Invitrogen) and controls were diluted to 1 ng input DNA to mimic DBS samples. Study
478 samples (mean DNA concentration 6.1±0.3 ng/µl) were not diluted. Target regions were amplified with
479 adjusted cycling conditions (1x99^{o}C-2min; 21x99^{o}C-15sec; 1x60^{o}C-8 min) in two reactions, and
480 subsequently combined for final library preparation according to the guidelines. Libraries were
481 quantified using KAPA Library Quantification Kit for Illumina Platforms (KAPA Biosystems), diluted to
482 2nM with low Tris-EDTA buffer, and pooled. Denatured library pool (18pM) was loaded on a Miseq
483 system (Illumina) for 2x300 paired-end sequencing (Miseq Reagent Kit v3, Illumina). A detailed protocol
484 is available at bio-protocol.org/###. 20% PhiX spike-in (Illumina) was used in one sequencing run to
485 determine the effect on sequencing quality and trade-off in coverage. Generated demultiplexed FASTQ
486 files were processed with an in-house analysis pipeline on a Unix operating system computer
487 (Supplementary file 3).

488 **Detection of *mdr1* and *pm2* copy number variations by PCR**

489 CNVs in *pm2* and *mdr1* were determined in a subset of samples (n=78) from all time periods and
490 districts using qPCR (94). Samples and controls were tested in triplicate with 20% of samples re-tested
491 for reproducibility with 100% of results in agreement.

492 **Analysis of Complexity of infection**

493 COI was estimated using the Real McCOIL categorical and proportional methods (101) in R using subsets
494 of variants: 1) all biallelic SNPs, 2) 25 barcode SNPs, 3) "core variants": biallelic variants excluding
495 repetitive regions (*i.e. hrp2*, *hrp3* and MS) and mitochondrial and apicoplast regions. Default settings
496 were used for a fixed error, and for the categorical method an upper bound of 10, and initial COI of 5
497 and for the proportional method an upper bound of 15, and initial COI of 7. We allowed 50%
498 missingness for biallelic SNPs, 20% for the barcode and 40% for core variants.

499 We also estimated the proportions of single and multiple clone infections based on the number of
500 heterozygous genotypes in 1) the 28-SNP barcode, 2) biallelic SNPs in *ama1*, and 3) core variants.
501 Samples with ≥1 heterozygous genotype were considered to contain multiple clones (COI≥2). Finally, we
502 estimated COI from the MS amplified regions. As the different methods generated diverging results, the
503 mode (most frequent value of single *vs.* multiple clone) was determined as final measure for each
504 sample.

505 **Validation of detection of *hrp2* and *hrp3* deletions**

506 The Pf AmpliSeq performance for *hrp2* and *hrp3* deletion detection was assessed in 10 previously-typed
507 samples (31). The presence or absence of both genes was determined using the mean read depth of
508 *hrp2* and *hrp3* amplicons (Supplementary file 3). Due to the repetitive nature and homologies between
509 *hrp2* and *hrp3* genes we used a conservative cut-off value, resulting in a "grey zone" where
510 deletion/presence was left inconclusive when the majority of amplicons were not in accordance. A final
511 variable for 'RDT-failure' (both *hrp2* and *hrp3* absent) *vs.* 'RDT-detectable' (*hrp2* and/or *hrp3* present)
512 was created, allowing the classification of samples that were inconclusive in one of the two genes if the
513 other gene was present.

514 **Population genetic analysis**

515 Population genetic analyses were performed using the 28-SNP barcode, excluding samples missing >7
516 SNPs (25%). Samples with heterozygous genotypes were included, justified by little genetic
517 differentiation (F_{ST}=0.05) between samples with single clone barcodes *vs.* samples with heterozygous
518 barcode genotypes. Genetic differentiation was measured as F_{ST} (102), $G`_{ST}$ (103) and Jost's D (104) using
519 1000 bootstraps with the R package DiveRsity (105). PCA was performed on the genotype matrix using
520 'prcomp' function (R stats package v4.0.5) using core variants. Prior to PCA, missing genotypes were
521 replaced by the mean allelic frequency at a locus in all samples. Expected heterozygosity (*He*) was
522 calculated (adegenet package (106, 107) in R) using diploid barcode genotypes. Wilcoxon signed-rank
523 test with continuity correction was used to compare mean observed heterozygosity (*Hobs)* to *He*. LD
524 was measured as the standardized index of association ($\bar{r}D$) in multilocus analysis using 999 resamplings
525 (method: permutation of alleles) using the poppr package v2.8.6. (108) in R. ML-lineages were defined
526 by grouping isolates with similar barcodes using the Hamming distance and clustered based on the
527 maximum distance (farthest neighbor) using poppr. DAPC (100) was performed with cross-validation,
528 and associated allele loadings for the first four components were determined.

529 **Analysis of genetic variants**

530 Barcode allele frequencies were calculated from allele depths to reflect population allele frequencies in
531 complex infections (Supplementary file 3). Haplotypes were created by combining genotypes of variants

532 of interest (Supplementary file 1). Frequency tables with confidence intervals were created with the
533 freqtables R-package.

534

535 **Data availability:**
536 Sample meta data and drug resistant and *hrp2* and *hrp3* haplotypes, barcodes, lineages location, date,
537 etc. is accessible at https://microreact.org/project/aV7RHNCBmG3sJ2rwzchE4k-peru-2003-2018-
538 molecular-surveillance-with-p-falciparum-ampliseq-assay. Raw data (fastq), variant files (vcf), and scripts
539 are available on request. All other data is included in the manuscript and supporting files.

540 **Acknowledgements:**
541 We wish to thank all clinical, microscopy and field staff who supported the sample collections and all
542 participants for making their material available for malaria studies. We acknowledge the support of the
543 Dirección Regional de Salud de Loreto for the study authorization and sample collection activities in
544 Loreto. The following reagents were obtained through BEI Resources, NIAID, NIH: *P. falciparum*, Strain
545 Dd2, MRA-150, contributed by David Walliker; *P. falciparum*, Strain Dd2_R539T, MRA-1255, and *P.*
546 *falciparum*, Strain CamWT_C580Y, MRA-1251, contributed by David A. Fidock; and *P. falciparum*, Strain
547 IPC 4912, MRA-1241, contributed by Didier Ménard.

548 **Funding:**
549 This work was funded by the Belgium Development Cooperation (DGD) under the Framework
550 Agreement Program between DGD and ITM (FA4 Peru, 2017-2021) and the sample collections in 2018
551 were supported by VLIR-UOS (project PE2018TEA470A102; University of Antwerp). Funding for the
552 sample collections lead by the U.S. Naval Medical Research Unit 6 (NAMRU-6) in 2011 and 2012 was
553 provided by the Armed Forces Health Surveillance Division (AFHSD) and its Global Emerging Infections
554 Surveillance and Response (GEIS) Section (P0144_20_N6_01, 2020-2021). Funding agencies had no role
555 in the design of the study.

556 **Competing interests**:

557 The authors declare that they have no competing interests.

558 **Copyright statement:**

559 Some authors of this manuscript are military service members and employees of the U.S. Government.
560 This work was prepared as part of their official duties. Title 17 U.S.C. §105 provides that "Copyright
561 protection under this Title is not available for any work of the United States Government". Title 17 U.S.C.
562 §101 defines a U.S. Government work as a work prepared by a military service member or employee of
563 the U.S. Government as part of that person's official duties. The views expressed in this article are those
564 of the authors and do not necessarily reflect the official policy or position of the Department of the
565 Navy, Department of Defense, nor the U.S. Government.

566 **Author contributions** (in alphabetical order per item): Conception of ideas for the study: ARU, DG, JHK;
567 Selection of targets and design of the assay: ERV, JHK, NvD; Sample collections and coordination of field
568 work: CDG, CFM, DG, HOV, JPvG; Laboratory experiments: CFM, JHK, NvD, PG; Bioinformatics & Data
569 analysis: JHK, LLA, NvD, PM; Writing first draft manuscript: ARU, JHK, CFM, NvD. All authors reviewed
570 and contributed to the final version of the manuscript.

571

572 **References**

573 1. WHO. 2019. World Malaria Report 2019. World Health Organization, Geneva.
574 2. Committee MPA. 2019. Technical consultation on the role of parasite and anopheline genetics in
575 malaria surveillance. World Health Organization, Geneva.
576 3. Dalmat R, Naughton B, Kwan-Gett TS, Slyker J, Stuckey EM. 2019. Use cases for genetic
577 epidemiology in malaria elimination. Malaria Journal 18:163.
578 4. WHO. 2018. Malaria Surveillance, Monitoring & Evaluation: A Reference Manual. World Health
579 Organization, Geneva.
580 5. WHO. 2009. Methods for surveillance of antimalarial drug efficacy. World Health Organization,
581 Geneva.
582 6. WHO. 2016. Minutes of the Evidence Review Group meeting on the emergence and spread of
583 multidrug-resistant Plasmodium falciparum lineages in the Greater Mekong subregion. . World
584 Health Organization, Geneva.
585 7. WHO. 2020. Report on antimalarial drug efficacy, resistance and response: 10 years of
586 surveillance (2010–2019). World Health Organization, Geneva.
587 8. Wangdi K, Pasaribu AP, Clements ACA. 2021. Addressing hard-to-reach populations for achieving
588 malaria elimination in the Asia Pacific Malaria Elimination Network countries. Asia & the Pacific
589 Policy Studies 8:176-188.
590 9. Ariey F, Witkowski B, Amaratunga C, Beghain J, Langlois AC, Khim N, Kim S, Duru V, Bouchier C,
591 Ma L, Lim P, Leang R, Duong S, Sreng S, Suon S, Chuor CM, Bout DM, Menard S, Rogers WO,
592 Genton B, Fandeur T, Miotto O, Ringwald P, Le Bras J, Berry A, Barale JC, Fairhurst RM, Benoit-
593 Vical F, Mercereau-Puijalon O, Menard D. 2014. A molecular marker of artemisinin-resistant
594 Plasmodium falciparum malaria. Nature 505:50-5.
595 10. Menard D, Khim N, Beghain J, Adegnika AA, Shafiul-Alam M, Amodu O, Rahim-Awab G, Barnadas
596 C, Berry A, Boum Y, Bustos MD, Cao J, Chen JH, Collet L, Cui L, Thakur GD, Dieye A, Djalle D,
597 Dorkenoo MA, Eboumbou-Moukoko CE, Espino FE, Fandeur T, Ferreira-da-Cruz MF, Fola AA,
598 Fuehrer HP, Hassan AM, Herrera S, Hongvanthong B, Houze S, Ibrahim ML, Jahirul-Karim M,
599 Jiang L, Kano S, Ali-Khan W, Khanthavong M, Kremsner PG, Lacerda M, Leang R, Leelawong M, Li
600 M, Lin K, Mazarati JB, Menard S, Morlais I, Muhindo-Mavoko H, Musset L, Na-Bangchang K,
601 Nambozi M, Niare K, Noedl H, et al. 2016. A Worldwide Map of Plasmodium falciparum K13-
602 Propeller Polymorphisms. N Engl J Med 374:2453-64.
603 11. Noedl H, Se Y, Schaecher K, Smith BL, Socheat D, Fukuda MM, Artemisinin Resistance in
604 Cambodia 1 Study C. 2008. Evidence of artemisinin-resistant malaria in western Cambodia. N
605 Engl J Med 359:2619-20.
606 12. Woodrow CJ, White NJ. 2017. The clinical impact of artemisinin resistance in Southeast Asia and
607 the potential for future spread. FEMS Microbiol Rev 41:34-48.
608 13. Balikagala B, Fukuda N, Ikeda M, Katuro OT, Tachibana S-I, Yamauchi M, Opio W, Emoto S,
609 Anywar DA, Kimura E, Palacpac NMQ, Odongo-Aginya EI, Ogwang M, Horii T, Mita T. 2021.
610 Evidence of Artemisinin-Resistant Malaria in Africa. New England Journal of Medicine 385:1163-
611 1171.
612 14. Programme WGM. 2019. WHO Malaria Policy Advisory Committee (MPAC) meeting - meeting
613 report. Geneva.
614 15. Mita T, Tanabe K, Kita K. 2009. Spread and evolution of Plasmodium falciparum drug resistance.
615 Parasitology International 58:201-209.
616 16. Auburn S, Barry AE. 2017. Dissecting malaria biology and epidemiology using population
617 genetics and genomics. Int J Parasitol 47:77-85.

618 17. Escalante AA, Ferreira MU, Vinetz JM, Volkman SK, Cui L, Gamboa D, Krogstad DJ, Barry AE,
619 Carlton JM, van Eijk AM, Pradhan K, Mueller I, Greenhouse B, Pacheco MA, Vallejo AF, Herrera S,
620 Felger I. 2015. Malaria Molecular Epidemiology: Lessons from the International Centers of
621 Excellence for Malaria Research Network. Am J Trop Med Hyg 93:79-86.
622 18. Gamboa D, Ho MF, Bendezu J, Torres K, Chiodini PL, Barnwell JW, Incardona S, Perkins M, Bell D,
623 McCarthy J, Cheng Q. 2010. A large proportion of P. falciparum isolates in the Amazon region of
624 Peru lack pfhrp2 and pfhrp3: implications for malaria rapid diagnostic tests. PLoS One 5:e8091.
625 19. Akinyi S, Hayden T, Gamboa D, Torres K, Bendezu J, Abdallah JF, Griffing SM, Quezada WM,
626 Arrospide N, De Oliveira AM, Lucas C, Magill AJ, Bacon DJ, Barnwell JW, Udhayakumar V. 2013.
627 Multiple genetic origins of histidine-rich protein 2 gene deletion in Plasmodium falciparum
628 parasites from Peru. Sci Rep 3:2797.
629 20. Murillo Solano C, Akinyi Okoth S, Abdallah JF, Pava Z, Dorado E, Incardona S, Huber CS, Macedo
630 de Oliveira A, Bell D, Udhayakumar V, Barnwell JW. 2015. Deletion of Plasmodium falciparum
631 Histidine-Rich Protein 2 (pfhrp2) and Histidine-Rich Protein 3 (pfhrp3) Genes in Colombian
632 Parasites. PLoS One 10:e0131576.
633 21. Dorado EJ, Okoth SA, Montenegro LM, Diaz G, Barnwell JW, Udhayakumar V, Murillo Solano C.
634 2016. Genetic Characterisation of Plasmodium falciparum Isolates with Deletion of the pfhrp2
635 and/or pfhrp3 Genes in Colombia: The Amazon Region, a Challenge for Malaria Diagnosis and
636 Control. PLoS One 11:e0163137.
637 22. Rachid Viana GM, Akinyi Okoth S, Silva-Flannery L, Lima Barbosa DR, Macedo de Oliveira A,
638 Goldman IF, Morton LC, Huber C, Anez A, Dantas Machado RL, Aranha Camargo LM, Costa
639 Negreiros do Valle S, Marins Póvoa M, Udhayakumar V, Barnwell JW. 2017. Histidine-rich
640 protein 2 (pfhrp2) and pfhrp3 gene deletions in Plasmodium falciparum isolates from select sites
641 in Brazil and Bolivia. PLoS One 12:e0171150.
642 23. Agaba BB, Yeka A, Nsobya S, Arinaitwe E, Nankabirwa J, Opigo J, Mbaka P, Lim CS, Kalyango JN,
643 Karamagi C, Kamya MR. 2019. Systematic review of the status of pfhrp2 and pfhrp3 gene
644 deletion, approaches and methods used for its estimation and reporting in Plasmodium
645 falciparum populations in Africa: review of published studies 2010–2019. Malaria Journal
646 18:355.
647 24. Thomson R, Parr JB, Cheng Q, Chenet S, Perkins M, Cunningham J. 2020. Prevalence of
648 Plasmodium falciparum lacking histidine-rich proteins 2 and 3: a systematic review. Bulletin of
649 the World Health Organization 98:558-568F.
650 25. WHO. 2021. Statement by the Malaria Policy Advisory Group on the urgent need to address the
651 high prevalence of pfhrp2/3 gene deletions in the Horn of Africa and beyond.
652 https://www.who.int/news/item/28-05-2021-statement-by-the-malaria-policy-advisory-group-
653 on-the-urgent-need-to-address-the-high-prevalence-of-pfhrp2-3-gene-deletions-in-the-horn-of-
654 africa-and-beyond. Accessed
655 26. Noviyanti R, Miotto O, Barry A, Marfurt J, Siegel S, Thuy-Nhien N, Quang HH, Anggraeni ND,
656 Laihad F, Liu Y, Sumiwi ME, Trimarsanto H, Coutrier F, Fadila N, Ghanchi N, Johora FT, Puspitasari
657 AM, Tavul L, Trianty L, Utami RAS, Wang D, Wangchuck K, Price RN, Auburn S. 2020.
658 Implementing parasite genotyping into national surveillance frameworks: feedback from control
659 programmes and researchers in the Asia-Pacific region. Malar J 19:271.
660 27. Fola AA, Harrison GLA, Hazairin MH, Barnadas C, Hetzel MW, Iga J, Siba PM, Mueller I, Barry AE.
661 2017. Higher Complexity of Infection and Genetic Diversity of Plasmodium vivax Than
662 Plasmodium falciparum Across All Malaria Transmission Zones of Papua New Guinea. Am J Trop
663 Med Hyg 96:630-641.
664 28. Fola AA, Nate E, Abby Harrison GL, Barnadas C, Hetzel MW, Iga J, Siba P, Mueller I, Barry AE.
665 2018. Nationwide genetic surveillance of Plasmodium vivax in Papua New Guinea reveals

666 heterogeneous transmission dynamics and routes of migration amongst subdivided populations.
667 Infect Genet Evol 58:83-95.
668 29. Waltmann A, Koepfli C, Tessier N, Karl S, Fola A, Darcy AW, Wini L, Harrison GLA, Barnadas C,
669 Jennison C, Karunajeewa H, Boyd S, Whittaker M, Kazura J, Bahlo M, Mueller I, Barry AE. 2018.
670 Increasingly inbred and fragmented populations of Plasmodium vivax associated with the
671 eastward decline in malaria transmission across the Southwest Pacific. PLoS Negl Trop Dis
672 12:e0006146.
673 30. Taylor SM, Parobek CM, Aragam N, Ngasala BE, Martensson A, Meshnick SR, Juliano JJ. 2013.
674 Pooled deep sequencing of Plasmodium falciparum isolates: an efficient and scalable tool to
675 quantify prevailing malaria drug-resistance genotypes. J Infect Dis 208:1998-2006.
676 31. Nsanzabana C, Djalle D, Guérin PJ, Ménard D, González IJ. 2018. Tools for surveillance of anti-
677 malarial drug resistance: an assessment of the current landscape. Malaria Journal 17:75.
678 32. Duraisingh MT, Curtis J, Warhurst DC. 1998. Plasmodium falciparum: detection of
679 polymorphisms in the dihydrofolate reductase and dihydropteroate synthetase genes by PCR
680 and restriction digestion. Exp Parasitol 89:1-8.
681 33. Eldin de Pecoulas P, Basco LK, Abdallah B, Dje MK, Le Bras J, Mazabraud A. 1995. Plasmodium
682 falciparum: detection of antifolate resistance by mutation-specific restriction enzyme digestion.
683 Exp Parasitol 80:483-7.
684 34. Talundzic E, Ravishankar S, Kelley J, Patel D, Plucinski M, Schmedes S, Ljolje D, Clemons B,
685 Madison-Antenucci S, Arguin PM, Lucchi NW, Vannberg F, Udhayakumar V. 2018. Next-
686 Generation Sequencing and Bioinformatics Protocol for Malaria Drug Resistance Marker
687 Surveillance. Antimicrobial Agents and Chemotherapy 62:e02474-17.
688 35. Baniecki ML, Faust AL, Schaffner SF, Park DJ, Galinsky K, Daniels RF, Hamilton E, Ferreira MU,
689 Karunaweera ND, Serre D, Zimmerman PA, Sa JM, Wellems TE, Musset L, Legrand E, Melnikov A,
690 Neafsey DE, Volkman SK, Wirth DF, Sabeti PC. 2015. Development of a single nucleotide
691 polymorphism barcode to genotype Plasmodium vivax infections. PLoS Negl Trop Dis
692 9:e0003539.
693 36. Daniels R, Volkman SK, Milner DA, Mahesh N, Neafsey DE, Park DJ, Rosen D, Angelino E, Sabeti
694 PC, Wirth DF, Wiegand RC. 2008. A general SNP-based molecular barcode for Plasmodium
695 falciparum identification and tracking. Malar J 7:223.
696 37. Fola AA, Kattenberg E, Razook Z, Lautu-Gumal D, Lee S, Mehra S, Bahlo M, Kazura J, Robinson LJ,
697 Laman M, Mueller I, Barry AE. 2020. SNP barcodes provide higher resolution than microsatellite
698 markers to measure Plasmodium vivax population genetics. Malar J 19:375.
699 38. Daniels RF, Schaffner SF, Wenger EA, Proctor JL, Chang H-H, Wong W, Baro N, Ndiaye D, Fall FB,
700 Ndiop M, Ba M, Milner DA, Taylor TE, Neafsey DE, Volkman SK, Eckhoff PA, Hartl DL, Wirth DF.
701 2015. Modeling malaria genomics reveals transmission decline and rebound in Senegal.
702 Proceedings of the National Academy of Sciences 112:7067-7072.
703 39. Taylor AR, Schaffner SF, Cerqueira GC, Nkhoma SC, Anderson TJC, Sriprawat K, Pyae Phyo A,
704 Nosten F, Neafsey DE, Buckee CO. 2017. Quantifying connectivity between local Plasmodium
705 falciparum malaria parasite populations using identity by descent. PLOS Genetics 13:e1007065.
706 40. Preston MD, Campino S, Assefa SA, Echeverry DF, Ocholla H, Amambua-Ngwa A, Stewart LB,
707 Conway DJ, Borrmann S, Michon P, Zongo I, Ouédraogo J-B, Djimde AA, Doumbo OK, Nosten F,
708 Pain A, Bousema T, Drakeley CJ, Fairhurst RM, Sutherland CJ, Roper C, Clark TG. 2014. A barcode
709 of organellar genome polymorphisms identifies the geographic origin of Plasmodium falciparum
710 strains. Nature Communications 5:4052.
711 41. Trimarsanto H, Amato R, Pearson RD, Sutanto E, Noviyanti R, Trianty L, Marfurt J, Pava Z,
712 Echeverry DF, Lopera-Mesa TM, Montenegro LM, Tobón-Castaño A, Grigg MJ, Barber B, William
713 T, Anstey NM, Getachew S, Petros B, Aseffa A, Assefa A, Rahim AG, Chau NH, Hien TT, Alam MS,

714 Khan WA, Ley B, Thriemer K, Wangchuck S, Hamedi Y, Adam I, Liu Y, Gao Q, Sriprawat K, Ferreira
715 MU, Barry A, Mueller I, Drury E, Goncalves S, Simpson V, Miotto O, Miles A, White NJ, Nosten F,
716 Kwiatkowski DP, Price RN, Auburn S. 2019. A molecular barcode and online tool to identify and
717 map imported infection with Plasmodium vivax. bioRxiv
718 doi:10.1101/776781:776781.
719 42. Jacob CG, Thuy-Nhien N, Mayxay M, Maude RJ, Quang HH, Hongvanthong B, Vanisaveth V, Duc
720 TN, Rekol H, van der Pluijm RW, Von Seidlein L, Fairhurst RM, Nosten FH, Hossain MA, Park N,
721 Goodwin S, Ringwald P, Chindavongsa K, Newton PN, Ashley EA, Phalivong S, Maude RR, Leang
722 R, Huch C, Dong LT, Nguyen K-T, Nhat TM, Hien TT, Nguyen H, Zdrojewski N, Canavati SE, Sayeed
723 AA, Uddin D, Buckee C, Fanello CI, Onyamboko M, Peto T, Tripura R, Amaratunga C, Thu AM,
724 Delmas G, Landier J, Parker DM, Chau NH, Lek D, Suon S, Callery JJ, Jittamala P,
725 Hanboonkunupakarn B, Pukrittayakamee S, et al. 2021. Genetic surveillance in the Greater
726 Mekong Subregion and South Asia to support malaria control and elimination. medRxiv.
727 43. Illumina. 2018. AmpliSeq for Illumina Custom and Community Panels: Reference Guide, San
728 Diego, California, USA.
729 44. WHO. 2020. World Malaria Report 2020. World Health Organization, Geneva.
730 45. Cortese JF, Caraballo A, Contreras CE, Plowe CV. 2002. Origin and dissemination of Plasmodium
731 falciparum drug-resistance mutations in South America. J Infect Dis 186:999-1006.
732 46. Chenet SM, Akinyi Okoth S, Huber CS, Chandrabose J, Lucchi NW, Talundzic E, Krishnalall K,
733 Ceron N, Musset L, Macedo de Oliveira A, Venkatesan M, Rahman R, Barnwell JW, Udhayakumar
734 V. 2016. Independent Emergence of the Plasmodium falciparum Kelch Propeller Domain Mutant
735 Allele C580Y in Guyana. J Infect Dis 213:1472-5.
736 47. Mathieu LC, Cox H, Early AM, Mok S, Lazrek Y, Paquet JC, Ade MP, Lucchi NW, Grant Q,
737 Udhayakumar V, Alexandre JS, Demar M, Ringwald P, Neafsey DE, Fidock DA, Musset L. 2020.
738 Local emergence in Amazonia of Plasmodium falciparum k13 C580Y mutants associated with in
739 vitro artemisinin resistance. Elife 9.
740 48. Vreden SG, Jitan JK, Bansie RD, Adhin MR. 2013. Evidence of an increased incidence of day 3
741 parasitaemia in Suriname: an indicator of the emerging resistance of Plasmodium falciparum to
742 artemether. Mem Inst Oswaldo Cruz 108:968-73.
743 49. Chenet SM, Okoth SA, Kelley J, Lucchi N, Huber CS, Vreden S, Macedo de Oliveira A, Barnwell
744 JW, Udhayakumar V, Adhin MR. 2017. Molecular Profile of Malaria Drug Resistance Markers of
745 Plasmodium falciparum in Suriname. Antimicrob Agents Chemother 61.
746 50. Rosas-Aguirre A, Erhart A, Llanos-Cuentas A, Branch O, Berkvens D, Abatih E, Lambert P, Frasso
747 G, Rodriguez H, Gamboa D, Sihuincha M, Rosanas-Urgell A, D'Alessandro U, Speybroeck N. 2015.
748 Modelling the potential of focal screening and treatment as elimination strategy for Plasmodium
749 falciparum malaria in the Peruvian Amazon Region. Parasit Vectors 8:261.
750 51. Anonymous. 1999. Política Nacional de Medicamentos para el Control de la Malaria en el Perú.
751 Ministerio de Salud del Perú, Lima, Perú.
752 52. Marquino W, MacArthur JR, Barat LM, Oblitas FE, Arrunategui M, Garavito G, Chafloque ML,
753 Pardave B, Gutierrez S, Arrospide N, Carrillo C, Cabezas C, Ruebush TK, 2nd. 2003. Efficacy of
754 chloroquine, sulfadoxine-pyrimethamine, and mefloquine for the treatment of uncomplicated
755 Plasmodium falciparum malaria on the north coast of Peru. Am J Trop Med Hyg 68:120-3.
756 53. Aramburú Guarda J, Ramal Asayag C, Witzig R. 1999. Malaria reemergence in the Peruvian
757 Amazon region. Emerg Infect Dis 5:209-15.
758 54. Ruebush TK, 2nd, Neyra D, Cabezas C. 2004. Modifying national malaria treatment policies in
759 Peru. J Public Health Policy 25:328-45.
760 55. Williams HA, Vincent-Mark A, Herrera Y, Chang OJ. 2009. A retrospective analysis of the change
761 in anti-malarial treatment policy: Peru. Malar J 8:85.

762 56. Marquino W, Huilca M, Calampa C, Falconi E, Cabezas C, Naupay R, Ruebush TK, 2nd. 2003.
763 Efficacy of mefloquine and a mefloquine-artesunate combination therapy for the treatment of
764 uncomplicated Plasmodium falciparum malaria in the Amazon Basin of Peru. Am J Trop Med Hyg
765 68:608-12.
766 57. de Oliveira AM, Chavez J, de Leon GP, Durand S, Arrospide N, Roberts J, Cabezas C, Marquino W.
767 2011. Efficacy and effectiveness of mefloquine and artesunate combination therapy for
768 uncomplicated Plasmodium falciparum malaria in the Peruvian Amazon. Am J Trop Med Hyg
769 85:573-8.
770 58. Anonymous. 2015. Norma téchnica de salud para la atencion de la malaria y malaria grave en el
771 Peru. Ministerio de Salud Perú, Direccion regional de Salud Loreto, Iquitos, Peru.
772 59. Rosas-Aguirre A, Speybroeck N, Llanos-Cuentas A, Rosanas-Urgell A, Carrasco-Escobar G,
773 Rodriguez H, Gamboa D, Contreras-Mancilla J, Alava F, Soares IS, Remarque E, U DA, Erhart A.
774 2015. Hotspots of Malaria Transmission in the Peruvian Amazon: Rapid Assessment through a
775 Parasitological and Serological Survey. PLoS One 10:e0137458.
776 60. Branch O, Casapia WM, Gamboa DV, Hernandez JN, Alava FF, Roncal N, Alvarez E, Perez EJ,
777 Gotuzzo E. 2005. Clustered local transmission and asymptomatic Plasmodium falciparum and
778 Plasmodium vivax malaria infections in a recently emerged, hypoendemic Peruvian Amazon
779 community. Malar J 4:27.
780 61. Lerch A, Koepfli C, Hofmann NE, Messerli C, Wilcox S, Kattenberg JH, Betuela I, O'Connor L,
781 Mueller I, Felger I. 2017. Development of amplicon deep sequencing markers and data analysis
782 pipeline for genotyping multi-clonal malaria infections. BMC Genomics 18:864.
783 62. Anderson TJ, Haubold B, Williams JT, Estrada-Franco JG, Richardson L, Mollinedo R, Bockarie M,
784 Mokili J, Mharakurwa S, French N, Whitworth J, Velez ID, Brockman AH, Nosten F, Ferreira MU,
785 Day KP. 2000. Microsatellite markers reveal a spectrum of population structures in the malaria
786 parasite Plasmodium falciparum. Mol Biol Evol 17:1467-82.
787 63. Koepfli C, Mueller I. 2017. Malaria Epidemiology at the Clone Level. Trends Parasitol 33:974-985.
788 64. Bacon DJ, McCollum AM, Griffing SM, Salas C, Soberon V, Santolalla M, Haley R, Tsukayama P,
789 Lucas C, Escalante AA, Udhayakumar V. 2009. Dynamics of malaria drug resistance patterns in
790 the Amazon basin region following changes in Peruvian national treatment policy for
791 uncomplicated malaria. Antimicrob Agents Chemother 53:2042-51.
792 65. Sridaran S, McClintock SK, Syphard LM, Herman KM, Barnwell JW, Udhayakumar V. 2010. Anti-
793 folate drug resistance in Africa: meta-analysis of reported dihydrofolate reductase (dhfr) and
794 dihydropteroate synthase (dhps) mutant genotype frequencies in African Plasmodium
795 falciparum parasite populations. Malar J 9:247.
796 66. Sidhu AB, Valderramos SG, Fidock DA. 2005. pfmdr1 mutations contribute to quinine resistance
797 and enhance mefloquine and artemisinin sensitivity in Plasmodium falciparum. Mol Microbiol
798 57:913-26.
799 67. Witkowski B, Duru V, Khim N, Ross LS, Saintpierre B, Beghain J, Chy S, Kim S, Ke S, Kloeung N,
800 Eam R, Khean C, Ken M, Loch K, Bouillon A, Domergue A, Ma L, Bouchier C, Leang R, Huy R, Nuel
801 G, Barale JC, Legrand E, Ringwald P, Fidock DA, Mercereau-Puijalon O, Ariey F, Menard D. 2017.
802 A surrogate marker of piperaquine-resistant Plasmodium falciparum malaria: a phenotype-
803 genotype association study. Lancet Infect Dis 17:174-183.
804 68. Price RN, Uhlemann AC, Brockman A, McGready R, Ashley E, Phaipun L, Patel R, Laing K,
805 Looareesuwan S, White NJ, Nosten F, Krishna S. 2004. Mefloquine resistance in Plasmodium
806 falciparum and increased pfmdr1 gene copy number. Lancet 364:438-447.
807 69. Veiga MI, Dhingra SK, Henrich PP, Straimer J, Gnadig N, Uhlemann AC, Martin RE, Lehane AM,
808 Fidock DA. 2016. Globally prevalent PfMDR1 mutations modulate Plasmodium falciparum
809 susceptibility to artemisinin-based combination therapies. Nat Commun 7:11553.

810 70. Tessema SK, Hathaway NJ, Teyssier NB, Murphy M, Chen A, Aydemir O, Duarte EM, Simone W,
811 Colborn J, Saute F, Crawford E, Aide P, Bailey JA, Greenhouse B. 2020. Sensitive, Highly
812 Multiplexed Sequencing of Microhaplotypes From the Plasmodium falciparum Heterozygome.
813 The Journal of Infectious Diseases doi:10.1093/infdis/jiaa527.
814 71. Jacob CG, Thuy-Nhien N, Mayxay M, Maude RJ, Quang HH, Hongvanthong B, Vanisaveth V, Ngo
815 Duc T, Rekol H, van der Pluijm R, von Seidlein L, Fairhurst R, Nosten F, Hossain MA, Park N,
816 Goodwin S, Ringwald P, Chindavongsa K, Newton P, Ashley E, Phalivong S, Maude R, Leang R,
817 Huch C, Dong LT, Nguyen K-T, Nhat TM, Hien TT, Nguyen H, Zdrojewski N, Canavati S, Sayeed AA,
818 Uddin D, Buckee C, Fanello CI, Onyamboko M, Peto T, Tripura R, Amaratunga C, Myint Thu A,
819 Delmas G, Landier J, Parker DM, Chau NH, Lek D, Suon S, Callery J, Jittamala P,
820 Hanboonkunupakarn B, Pukrittayakamee S, et al. 2021. Genetic surveillance in the Greater
821 Mekong subregion and South Asia to support malaria control and elimination. eLife 10:e62997.
822 72. Henriques G, Hallett RL, Beshir KB, Gadalla NB, Johnson RE, Burrow R, van Schalkwyk DA, Sawa
823 P, Omar SA, Clark TG, Bousema T, Sutherland CJ. 2014. Directional selection at the pfmdr1, pfcrt,
824 pfubp1, and pfap2mu loci of Plasmodium falciparum in Kenyan children treated with ACT. J
825 Infect Dis 210:2001-8.
826 73. Cerqueira GC, Cheeseman IH, Schaffner SF, Nair S, McDew-White M, Phyo AP, Ashley EA,
827 Melnikov A, Rogov P, Birren BW, Nosten F, Anderson TJC, Neafsey DE. 2017. Longitudinal
828 genomic surveillance of Plasmodium falciparum malaria parasites reveals complex genomic
829 architecture of emerging artemisinin resistance. Genome Biology 18:78.
830 74. Xie SC, Ralph SA, Tilley L. 2020. K13, the Cytostome, and Artemisinin Resistance. Trends in
831 Parasitology 36:533-544.
832 75. Birnbaum J, Scharf S, Schmidt S, Jonscher E, Hoeijmakers WAM, Flemming S, Toenhake CG,
833 Schmitt M, Sabitzki R, Bergmann B, Frohlke U, Mesen-Ramirez P, Blancke Soares A, Herrmann H,
834 Bartfai R, Spielmann T. 2020. A Kelch13-defined endocytosis pathway mediates artemisinin
835 resistance in malaria parasites. Science 367:51-59.
836 76. Henrici RC, Edwards RL, Zoltner M, van Schalkwyk DA, Hart MN, Mohring F, Moon RW, Nofal SD,
837 Patel A, Flueck C, Baker DA, John ARO, Field MC, Sutherland CJ. 2020. The Plasmodium
838 falciparum Artemisinin Susceptibility-Associated AP-2 Adaptin mu Subunit is Clathrin
839 Independent and Essential for Schizont Maturation. Mbio 11.
840 77. Behrens HM, Schmidt S, Spielmann T. 2021. The newly discovered role of endocytosis in
841 artemisinin resistance. Medicinal Research Reviews 41:2998-3022.
842 78. Sutherland CJ, Henrici RC, Artavanis-Tsakonas K. 2021. Artemisinin susceptibility in the malaria
843 parasite Plasmodium falciparum: propellers, adaptor proteins and the need for cellular healing.
844 FEMS Microbiol Rev 45.
845 79. Demas AR, Sharma AI, Wong W, Early AM, Redmond S, Bopp S, Neafsey DE, Volkman SK, Hartl
846 DL, Wirth DF. 2018. Mutations in Plasmodium falciparum actin-binding protein coronin confer
847 reduced artemisinin susceptibility. Proc Natl Acad Sci U S A doi:10.1073/pnas.1812317115.
848 80. Velavan TP, Nderu D, Agbenyega T, Ntoumi F, Kremsner PG. 2019. An alternative dogma on
849 reduced artemisinin susceptibility: A new shadow from east to west. Proceedings of the National
850 Academy of Sciences 116:12611-12612.
851 81. Sharma AI, Shin SH, Bopp S, Volkman SK, Hartl DL, Wirth DF. 2020. Genetic background and
852 PfKelch13 affect artemisinin susceptibility of PfCoronin mutants in Plasmodium falciparum. PLoS
853 Genet 16:e1009266.
854 82. Oberstaller J, Zoungrana L, Bannerman CD, Jahangiri S, Dwivedi A, Silva JC, Adams JH, Takala-
855 Harrison S. 2021. Integration of population and functional genomics to understand mechanisms
856 of artemisinin resistance in Plasmodium falciparum. International Journal for Parasitology: Drugs
857 and Drug Resistance 16:119-128.

858 83. Griffing SM, Mixson-Hayden T, Sridaran S, Alam MT, McCollum AM, Cabezas C, Marquino
859 Quezada W, Barnwell JW, De Oliveira AM, Lucas C, Arrospide N, Escalante AA, Bacon DJ,
860 Udhayakumar V. 2011. South American Plasmodium falciparum after the malaria eradication
861 era: clonal population expansion and survival of the fittest hybrids. PLoS One 6:e23486.
862 84. Baldeviano GC, Okoth SA, Arrospide N, Gonzalez RV, Sanchez JF, Macedo S, Conde S, Tapia LL,
863 Salas C, Gamboa D, Herrera Y, Edgel KA, Udhayakumar V, Lescano AG. 2015. Molecular
864 Epidemiology of Plasmodium falciparum Malaria Outbreak, Tumbes, Peru, 2010-2012. Emerg
865 Infect Dis 21:797-803.
866 85. Okoth SA, Chenet SM, Arrospide N, Gutierrez S, Cabezas C, Matta JA, Udhayakumar V. 2016.
867 Molecular Investigation into a Malaria Outbreak in Cusco, Peru: Plasmodium falciparum BV1
868 Lineage is Linked to a Second Outbreak in Recent Times. Am J Trop Med Hyg 94:128-31.
869 86. Recht J, Siqueira AM, Monteiro WM, Herrera SM, Herrera S, Lacerda MVG. 2017. Malaria in
870 Brazil, Colombia, Peru and Venezuela: current challenges in malaria control and elimination.
871 Malaria Journal 16:273.
872 87. Villena FE, Lizewski SE, Joya CA, Valdivia HO. 2021. Population genomics and evidence of clonal
873 replacement of Plasmodium falciparum in the Peruvian Amazon. Scientific Reports 11:21212.
874 88. Schmedes SE, Patel D, Kelley J, Udhayakumar V, Talundzic E. 2019. Using the Plasmodium
875 mitochondrial genome for classifying mixed-species infections and inferring the geographical
876 origin of P. falciparum parasites imported to the U.S. PLOS ONE 14:e0215754.
877 89. Hathaway NJ, Parobek CM, Juliano JJ, Bailey JA. 2017. SeekDeep: single-base resolution de novo
878 clustering for amplicon deep sequencing. Nucleic Acids Research 46:e21-e21.
879 90. Callahan BJ, McMurdie PJ, Rosen MJ, Han AW, Johnson AJA, Holmes SP. 2016. DADA2: High-
880 resolution sample inference from Illumina amplicon data. Nature Methods 13:581-583.
881 91. Henden L, Lee S, Mueller I, Barry A, Bahlo M. 2018. Identity-by-descent analyses for measuring
882 population dynamics and selection in recombining pathogens. PLoS Genet 14:e1007279.
883 92. Grande T, Bernasconi A, Erhart A, Gamboa D, Casapia M, Delgado C, Torres K, Fanello C, Llanos-
884 Cuentas A, D'Alessandro U. 2007. A Randomised Controlled Trial to Assess the Efficacy of
885 Dihydroartemisinin-Piperaquine for the Treatment of Uncomplicated Falciparum Malaria in
886 Peru. PLOS ONE 2:e1101.
887 93. Mangold KA, Manson RU, Koay ES, Stephens L, Regner M, Thomson RB, Jr., Peterson LR, Kaul KL.
888 2005. Real-time PCR for detection and identification of Plasmodium spp. J Clin Microbiol
889 43:2435-40.
890 94. Rovira-Vallbona E, Van Hong N, Kattenberg JH, Huan RM, Hien NTT, Ngoc NTH, Guetens P, Hieu
891 NL, Mai TT, Duong NTT, Duong TT, Phuc BQ, Xa NX, Erhart A, Rosanas-Urgell A. 2020. Efficacy of
892 dihydroartemisinin/piperaquine and artesunate monotherapy for the treatment of
893 uncomplicated Plasmodium falciparum malaria in Central Vietnam. J Antimicrob Chemother
894 75:2272-2281.
895 95. Oyola SO, Ariani CV, Hamilton WL, Kekre M, Amenga-Etego LN, Ghansah A, Rutledge GG,
896 Redmond S, Manske M, Jyothi D, Jacob CG, Otto TD, Rockett K, Newbold CI, Berriman M,
897 Kwiatkowski DP. 2016. Whole genome sequencing of Plasmodium falciparum from dried blood
898 spots using selective whole genome amplification. Malar J 15:597.
899 96. Straimer J, Gnädig NF, Witkowski B, Amaratunga C, Duru V, Ramadani AP, Dacheux M, Khim N,
900 Zhang L, Lam S, Gregory PD, Urnov FD, Mercereau-Puijalon O, Benoit-Vical F, Fairhurst RM,
901 Ménard D, Fidock DA. 2015. Drug resistance. K13-propeller mutations confer artemisinin
902 resistance in Plasmodium falciparum clinical isolates. Science 347:428-31.
903 97. Miotto O, Sekihara M, Tachibana S-I, Yamauchi M, Pearson RD, Amato R, Gonçalves S, Mehra S,
904 Noviyanti R, Marfurt J, Auburn S, Price RN, Mueller I, Ikeda M, Mori T, Hirai M, Tavul L, Hetzel
905 MW, Laman M, Barry AE, Ringwald P, Ohashi J, Hombhanje F, Kwiatkowski DP, Mita T. 2020.

906 Emergence of artemisinin-resistant Plasmodium falciparum with kelch13 C580Y mutations on
907 the island of New Guinea. PLOS Pathogens 16:e1009133.
908 98. Ross LS, Dhingra SK, Mok S, Yeo T, Wicht KJ, Kumpornsin K, Takala-Harrison S, Witkowski B,
909 Fairhurst RM, Ariey F, Menard D, Fidock DA. 2018. Emerging Southeast Asian PfCRT mutations
910 confer Plasmodium falciparum resistance to the first-line antimalarial piperaquine. Nat Commun
911 9:3314.
912 99. MalariaGEN. 2015. MalariaGEN Plasmodium falciparum Community Project, *on* MRC Centre for
913 Genomics and Global Health. https://www.malariagen.net/apps/pf/4.0/. Accessed
914 100. Jombart T, Devillard S, Balloux F. 2010. Discriminant analysis of principal components: a new
915 method for the analysis of genetically structured populations. BMC Genet 11:94.
916 101. Chang HH, Worby CJ, Yeka A, Nankabirwa J, Kamya MR, Staedke SG, Dorsey G, Murphy M,
917 Neafsey DE, Jeffreys AE, Hubbart C, Rockett KA, Amato R, Kwiatkowski DP, Buckee CO,
918 Greenhouse B. 2017. THE REAL McCOIL: A method for the concurrent estimation of the
919 complexity of infection and SNP allele frequency for malaria parasites. PLoS Comput Biol
920 13:e1005348.
921 102. Weir BS, Cockerham CC. 1984. Estimating F-Statistics for the Analysis of Population Structure.
922 Evolution 38:1358-1370.
923 103. Hedrick PW. 2005. A standardized genetic differentiation measure. Evolution 59:1633-8.
924 104. Jost L. 2008. G(ST) and its relatives do not measure differentiation. Mol Ecol 17:4015-26.
925 105. Keenan K, McGinnity P, Cross TF, Crozier WW, Prodöhl PA. 2013. diveRsity: An R package for the
926 estimation and exploration of population genetics parameters and their associated errors.
927 Methods in Ecology and Evolution 4:782-788.
928 106. Jombart T. 2008. adegenet: a R package for the multivariate analysis of genetic markers.
929 Bioinformatics 24:1403-5.
930 107. Jombart T, Ahmed I. 2011. adegenet 1.3-1: new tools for the analysis of genome-wide SNP data.
931 Bioinformatics 27:3070-1.
932 108. Kamvar ZN, Tabima JF, Grunwald NJ. 2014. Poppr: an R package for genetic analysis of
933 populations with clonal, partially clonal, and/or sexual reproduction. PeerJ 2:e281.
934 109. Henriques G, van Schalkwyk DA, Burrow R, Warhurst DC, Thompson E, Baker DA, Fidock DA,
935 Hallett R, Flueck C, Sutherland CJ. 2015. The Mu subunit of Plasmodium falciparum clathrin-
936 associated adaptor protein 2 modulates in vitro parasite response to artemisinin and quinine.
937 Antimicrob Agents Chemother 59:2540-7.
938 110. Adams T, Ennuson NAA, Quashie NB, Futagbi G, Matrevi S, Hagan OCK, Abuaku B, Koram KA,
939 Duah NO. 2018. Prevalence of Plasmodium falciparum delayed clearance associated
940 polymorphisms in adaptor protein complex 2 mu subunit (pfap2mu) and ubiquitin specific
941 protease 1 (pfubp1) genes in Ghanaian isolates. Parasit Vectors 11:175.
942 111. Martin RE, Marchetti RV, Cowan AI, Howitt SM, Broer S, Kirk K. 2009. Chloroquine transport via
943 the malaria parasite's chloroquine resistance transporter. Science 325:1680-2.
944 112. Sidhu AB, Verdier-Pinard D, Fidock DA. 2002. Chloroquine resistance in Plasmodium falciparum
945 malaria parasites conferred by pfcrt mutations. Science 298:210-3.
946 113. Fidock DA, Nomura T, Talley AK, Cooper RA, Dzekunov SM, Ferdig MT, Ursos LM, Sidhu AB,
947 Naude B, Deitsch KW, Su XZ, Wootton JC, Roepe PD, Wellems TE. 2000. Mutations in the P.
948 falciparum digestive vacuole transmembrane protein PfCRT and evidence for their role in
949 chloroquine resistance. Mol Cell 6:861-71.
950 114. Nagesha HS, Casey GJ, Rieckmann KH, Fryauff DJ, Laksana BS, Reeder JC, Maguire JD, Baird JK.
951 2003. NEW HAPLOTYPES OF THE PLASMODIUM FALCIPARUM CHLOROQUINE RESISTANCE
952 TRANSPORTER (PFCRT) GENE AMONG CHLOROQUINE-RESISTANT PARASITE ISOLATES. The
953 American Journal of Tropical Medicine and Hygiene Am J Trop Med Hyg 68:398-402.

954 115. Roepe PD. 2009. Molecular and physiologic basis of quinoline drug resistance in Plasmodium
955 falciparum malaria. Future Microbiology 4:441-455.
956 116. Dhingra SK, Redhi D, Combrinck JM, Yeo T, Okombo J, Henrich PP, Cowell AN, Gupta P, Stegman
957 ML, Hoke JM, Cooper RA, Winzeler E, Mok S, Egan TJ, Fidock DA. 2017. A Variant PfCRT Isoform
958 Can Contribute to Plasmodium falciparum Resistance to the First-Line Partner Drug Piperaquine.
959 MBio 8.
960 117. Hamilton WL, Amato R, van der Pluijm RW, Jacob CG, Quang HH, Thuy-Nhien NT, Hien TT,
961 Hongvanthong B, Chindavongsa K, Mayxay M, Huy R, Leang R, Huch C, Dysoley L, Amaratunga C,
962 Suon S, Fairhurst RM, Tripura R, Peto TJ, Sovann Y, Jittamala P, Hanboonkunupakarn B,
963 Pukrittayakamee S, Chau NH, Imwong M, Dhorda M, Vongpromek R, Chan XHS, Maude RJ,
964 Pearson RD, Nguyen T, Rockett K, Drury E, Gonçalves S, White NJ, Day NP, Kwiatkowski DP,
965 Dondorp AM, Miotto O. 2019. Evolution and expansion of multidrug-resistant malaria in
966 southeast Asia: a genomic epidemiology study. The Lancet Infectious Diseases 19:943-951.
967 118. Pelleau S, Moss EL, Dhingra SK, Volney B, Casteras J, Gabryszewski SJ, Volkman SK, Wirth DF,
968 Legrand E, Fidock DA, Neafsey DE, Musset L. 2015. Adaptive evolution of malaria parasites in
969 French Guiana: Reversal of chloroquine resistance by acquisition of a mutation in
970 pfcrt. Proceedings of the National Academy of Sciences 112:11672-11677.
971 119. van der Pluijm RW, Imwong M, Chau NH, Hoa NT, Thuy-Nhien NT, Thanh NV, Jittamala P,
972 Hanboonkunupakarn B, Chutasmit K, Saelow C, Runjarern R, Kaewmok W, Tripura R, Peto TJ, Yok
973 S, Suon S, Sreng S, Mao S, Oun S, Yen S, Amaratunga C, Lek D, Huy R, Dhorda M, Chotivanich K,
974 Ashley EA, Mukaka M, Waithira N, Cheah PY, Maude RJ, Amato R, Pearson RD, Gonçalves S,
975 Jacob CG, Hamilton WL, Fairhurst RM, Tarning J, Winterberg M, Kwiatkowski DP,
976 Pukrittayakamee S, Hien TT, Day NP, Miotto O, White NJ, Dondorp AM. 2019. Determinants of
977 dihydroartemisinin-piperaquine treatment failure in Plasmodium falciparum malaria in
978 Cambodia, Thailand, and Vietnam: a prospective clinical, pharmacological, and genetic study.
979 Lancet Infect Dis 19:952-961.
980 120. Folarin OA, Bustamante C, Gbotosho GO, Sowunmi A, Zalis MG, Oduola AM, Happi CT. 2011. In
981 vitro amodiaquine resistance and its association with mutations in pfcrt and pfmdr1 genes of
982 Plasmodium falciparum isolates from Nigeria. Acta Trop 120:224-30.
983 121. Korsinczky M, Chen N, Kotecka B, Saul A, Rieckmann K, Cheng Q. 2000. Mutations in Plasmodium
984 falciparum cytochrome b that are associated with atovaquone resistance are located at a
985 putative drug-binding site. Antimicrob Agents Chemother 44:2100-8.
986 122. Akhoon BA, Singh KP, Varshney M, Gupta SK, Shukla Y, Gupta SK. 2014. Understanding the
987 mechanism of atovaquone drug resistance in Plasmodium falciparum cytochrome b mutation
988 Y268S using computational methods. PLoS One 9:e110041.
989 123. Peters JM, Chen N, Gatton M, Korsinczky M, Fowler EV, Manzetti S, Saul A, Cheng Q. 2002.
990 Mutations in cytochrome b resulting in atovaquone resistance are associated with loss of fitness
991 in Plasmodium falciparum. Antimicrob Agents Chemother 46:2435-41.
992 124. Griffing SM, Viana GM, Mixson-Hayden T, Sridaran S, Alam MT, de Oliveira AM, Barnwell JW,
993 Escalante AA, Povoa MM, Udhayakumar V. 2013. Historical shifts in Brazilian P. falciparum
994 population structure and drug resistance alleles. PLoS One 8:e58984.
995 125. Costa GL, Amaral LC, Fontes CJF, Carvalho LH, de Brito CFA, de Sousa TN. 2017. Assessment of
996 copy number variation in genes related to drug resistance in Plasmodium vivax and Plasmodium
997 falciparum isolates from the Brazilian Amazon and a systematic review of the literature. Malar J
998 16:152.
999 126. Basco LK, Ringwald P. 2000. Molecular epidemiology of malaria in Yaounde, Cameroon. VI.
1000 Sequence variations in the Plasmodium falciparum dihydrofolate reductase-thymidylate

1001 synthase gene and in vitro resistance to pyrimethamine and cycloguanil. The American journal
1002 of tropical medicine and hygiene Am J Trop Med Hyg Am J Trop Med Hyg 62:271-276.
1003 127. Hyde JE. 2007. Drug-resistant malaria – an insight. The FEBS Journal 274:4688-4698.
1004 128. Staines HM, Burrow R, Teo BH-Y, Chis Ster I, Kremsner PG, Krishna S. 2017. Clinical implications
1005 of Plasmodium resistance to atovaquone/proguanil: a systematic review and meta-analysis.
1006 Journal of Antimicrobial Chemotherapy 73:581-595.
1007 129. Amato R, Lim P, Miotto O, Amaratunga C, Dek D, Pearson RD, Almagro-Garcia J, Neal AT, Sreng
1008 S, Suon S, Drury E, Jyothi D, Stalker J, Kwiatkowski DP, Fairhurst RM. 2017. Genetic markers
1009 associated with dihydroartemisinin-piperaquine failure in Plasmodium falciparum malaria in
1010 Cambodia: a genotype-phenotype association study. Lancet Infect Dis 17:164-173.
1011 130. Reed MB, Saliba KJ, Caruana SR, Kirk K, Cowman AF. 2000. Pgh1 modulates sensitivity and
1012 resistance to multiple antimalarials in Plasmodium falciparum. Nature 403:906-909.
1013 131. Pickard Amy L, Wongsrichanalai C, Purfield A, Kamwendo D, Emery K, Zalewski C, Kawamoto F,
1014 Miller RS, Meshnick Steven R. 2003. Resistance to Antimalarials in Southeast Asia and Genetic
1015 Polymorphisms in pfmdr1. Antimicrobial Agents and Chemotherapy 47:2418-2423.
1016 132. Mbaye A, Dieye B, Ndiaye YD, Bei AK, Muna A, Deme AB, Yade MS, Diongue K, Gaye A, Ndiaye
1017 IM, Ndiaye T, Sy M, Diallo MA, Badiane AS, Ndiaye M, Seck MC, Sy N, Koita O, Krogstad DJ,
1018 Nwakanma D, Ndiaye D. 2016. Selection of N86F184D1246 haplotype of Pfmrd1 gene by
1019 artemether-lumefantrine drug pressure on Plasmodium falciparum populations in Senegal.
1020 Malar J 15:433.
1021 133. Venkatesan M, Gadalla NB, Stepniewska K, Dahal P, Nsanzabana C, Moriera C, Price RN,
1022 Martensson A, Rosenthal PJ, Dorsey G, Sutherland CJ, Guerin P, Davis TM, Menard D, Adam I,
1023 Ademowo G, Arze C, Baliraine FN, Berens-Riha N, Bjorkman A, Borrmann S, Checchi F, Desai M,
1024 Dhorda M, Djimde AA, El-Sayed BB, Eshetu T, Eyase F, Falade C, Faucher JF, Froberg G,
1025 Grivoyannis A, Hamour S, Houze S, Johnson J, Kamugisha E, Kariuki S, Kiechel JR, Kironde F,
1026 Kofoed PE, LeBras J, Malmberg M, Mwai L, Ngasala B, Nosten F, Nsobya SL, Nzila A, Oguike M,
1027 Otienoburu SD, Ogutu B, et al. 2014. Polymorphisms in Plasmodium falciparum chloroquine
1028 resistance transporter and multidrug resistance 1 genes: parasite risk factors that affect
1029 treatment outcomes for P. falciparum malaria after artemether-lumefantrine and artesunate-
1030 amodiaquine. Am J Trop Med Hyg 91:833-43.
1031 134. Dahlstrom S, Ferreira PE, Veiga MI, Sedighi N, Wiklund L, Martensson A, Farnert A, Sisowath C,
1032 Osorio L, Darban H, Andersson B, Kaneko A, Conseil G, Bjorkman A, Gil JP. 2009. Plasmodium
1033 falciparum multidrug resistance protein 1 and artemisinin-based combination therapy in Africa. J
1034 Infect Dis 200:1456-64.
1035 135. Bopp S, Magistrado P, Wong W, Schaffner SF, Mukherjee A, Lim P, Dhorda M, Amaratunga C,
1036 Woodrow CJ, Ashley EA, White NJ, Dondorp AM, Fairhurst RM, Ariey F, Menard D, Wirth DF,
1037 Volkman SK. 2018. Plasmepsin II-III copy number accounts for bimodal piperaquine resistance
1038 among Cambodian Plasmodium falciparum. Nat Commun 9:1769.
1039 136. Dharia NV, Plouffe D, Bopp SE, Gonzalez-Paez GE, Lucas C, Salas C, Soberon V, Bursulaya B,
1040 Kochel TJ, Bacon DJ, Winzeler EA. 2010. Genome scanning of Amazonian Plasmodium falciparum
1041 shows subtelomeric instability and clindamycin-resistant parasites. Genome Res 20:1534-44.

1042

1043

1044 ## Tables

1045 **Table 1. Genes of interest for drug resistance molecular surveillance of malaria in Peru.**

Gene ID	Chromosome	Gene with resistance-associated SNP(s)	Drug associated with resistance*
PF3D7_1218300	12	*ap2-mu*	ART (72, 76, 109, 110); QN (109)
PF3D7_1251200	12	*coronin*	DHA (79, 81)
PF3D7_0709000	7	*crt*	CQ (111-115); PPQ (98, 116-119); AMQ (120)
mal_mito_3	mitochondrial	*cytochrome B*	ATQ (121-123)
PF3D7_0417200	4	*dhfr*	PYR (64, 83, 124-127); PG (128)
PF3D7_0810800	8	*dhps*	SULF (64, 83, 124, 125, 127)
PF3D7_1362500	13	*exonuclease*	PPQ (129)
PF3D7_1343700	13	*k13*	ART (9, 46)
PF3D7_0523000	5	*mdr1*	CQ (130, 131); PPQ (69); MQ (68), QN, HF, ART (64, 66, 68, 69, 125, 132); AMQ (69, 120); LF (132, 133)
PF3D7_0112200	1	*mrp1*	ART, MQ, LF (69, 134)
PF3D7_1408000	14	*plasmepsin II*	PPQ (67, 129, 135)
PF3D7_API04900	apicoplast	*23s rRNA*	CM (136)
PF3D7_0104300	1	*ubp-1*	ART (72, 75, 109, 110)

1046 *AMQ: amodiaquine; ART: artesunate; ATQ: atovaquone; CM: clindamycin; CQ: chloroquine; DHA: dihydroartemisinin; HF:*
1047 *halofantrine; LF: lumefantrine; MQ: mefloquine; PG: proguanil; PPQ: piperaquine; PYR: pyrimethamine; SULF: sulfadoxine; QN:*
1048 *quinine. *The list of drugs to which resistance has been observed is non-exhaustive. Validated mutations are listed in the WHO*
1049 *Report on antimalarial drug efficacy, resistance and response: 10 years of surveillance (2010–2019) (7)*

Table 2. Barcode multilocus lineage characteristics. ML lineages were identified, clustered using genetic distance between barcodes with the poppr package in R, and given a number as identifier. Heterozygote genotypes in the barcode were included, resulting in the creating of some mixed clones barcodes, which include lineages in other lineages. Lineage 29 and 95 are in fact the same as lineage 155, with additional minor clones.

Barcode multilocus lineage		2003-2005			2008-2012		2014-2018			variants of interest for drug resistance							HRP2/HRP3 both deleted (RDT failure)
		unknown district	Belen	San Juan Bautista	Punchana	San Juan Bautista	Mazan	San Juan Bautista	Pastaza	dhfr	dhps	crt	mdr1	coronin	K13	ubp1 - category	
53	GGTGTCTATCTCATCGCGGGGTTTCATC	0	**1**	**19**	0	0	0	0	0	single_mutant	*wt*	CVMNT	NDFCDD	V424I	K189T	Q107L and/or K1193T variant	no
142	GGTGTCTATTTCGGTTAGGAGTTTCATC	0	0	**19**	0	0	0	0	0	single_mutant	single_syn_mutant_540	CVMNT	NDFCDD	V424I	K189T	R1133S variant	no
148	AGTGTCCGTCCAATCGCGGGATTTTTTC	0	0	**16**	0	0	0	0	0	double_mutant	*wt*	SVMNT	NGFSDD	*wt*	*wt*	R1133S variant	no
141	GGCGCCCGTCCAATCGCCGGATTACTACC	0	0	**10**	0	0	0	0	0	double_mutant	double_mutant	SVMNT	NDFCDY	*wt*	K189T	R1133S + E1011K variant	no (9)/**yes (1)**
124	GGTGCCCGTCCCATCGCCGGATTTTTTC	0	0	**3**	0	0	0	0	0	double_mutant	double_mutant/triple_mutant	SVMNT	NDFCDY	V424I/ *wt*	*wt*	Q107L and/or K1193T variant	no
140	GGTGTCTATCTCATCGCGGGACTTCATC	0	0	**3**	0	0	0	0	0	single_mutant	*wt*	CVMNT	NGFSDD	V424I	K189T	Q107L and/or K1193T variant	no
146	GGTXXCTATCTCATCGXGGGGCTTCATC	0	0	**2**	0	0	0	0	0	single_mutant	*wt* incomplete	CVMNT	mixed	V424I	*wt* incomplete	Q107L and/or K1193T variant	no
161	GGTGCCCXTCCCATCGCCGGATTATTACC	0	0	**2**	0	0	0	0	0	double_mutant	double_mutant/triple_mutant	SVMNT	NDFCDY	V424I/ *wt*	K189T		no
62	GGCGCCTATCTCATCGCGGGATTTTACC	0	0	**1**	0	0	0	0	0	single_mutant	*wt*	CVMNT	NDFCDY	V424I	K189T		no
63	GGCGCCTATCTAATXGCCGGATTATNATC	0	0	**1**	0	0	0	0	0	single_mutant	incomplete_mut	CVMNT	mixed	V424I	K189T	mixed	
100	GGXGXCTGXCCXGGXNCXGGATTANTANC	0	0	**1**	0	0	0	0	0	single_mutant	incomplete_mut	CVMNT	NDFCDD	V424I	K189T	mixed	no
104	GGXGXCTATCTXGGTTXXGAGTTCCACT	0	0	**1**	0	0	0	0	0	single_mutant	*wt*	CVMNT	NDFCDD	V62M	K189T	R1133S variant	no

119	GGXXXCTXTNTXNTNGXXXXGTTXCXTC	0	0	**1**	0	0	0	0	0		single_mutant		NDFCDD	V424I	G449C	incomplete only *wt*	no
121	GGXXXCCGTTTXATTGXXGGATTACCACC	0	0	**1**	0	0	0	0	0	double_mutant	*wt*	SVMNT	NGFSDD	V62M	K189T	R1133S variant	no
131	GAXAXTTAXCCXGGCTXXGAACTATCATT	0	0	**1**	0	0	0	0	0	*wt*	*wt*	CVMNT	NDFSDD	V62M	*wt* incomplete	R1133S + E1011K variant	no
133	GXXGXCTAXTTXATCGNXGGGTTTCATC	0	0	**1**	0	0	0	0	0	single_mutant	*wt*	CVMNT	NDFCDD	V424I	K189T	incomplete only *wt*	no
136	GXXXXCTAXTTXGTTXXXGAGXTCCAXC	0	0	**1**	0	0	0	0	0		*wt* incomplete	CVMNT	incomplete	V62M	*wt* incomplete	incomplete only *wt*	**yes**
144	XGTXCXTXTXXCXTCTXCXGATTAXCXTC	0	0	**1**	0	0	0	0	0	incomplete_mutant	double_mutant		incomplete	*wt*	*wt* incomplete		no
162	XACXCXTXTXTCXGTTXGXAGCTAXCXTT	0	0	**1**	0	0	0	0	0	single_mutant	single_syn_mutant_540		NG_SDD	V62M			no
163	XAXXXCNXTTXXNTTTXGXAGTTXTXTC	0	**1**	0	0	0	0	0	0	*wt*	*wt* incomplete		mixed	V62M	*wt* incomplete	incomplete only *wt*	no
157	GGCGCCTATCCCATCGCCGGGTTACTACC	0	0	**29**	0	**2**	0	0	0	single_mutant	*wt*	SVMNT	NDFCDD	V424I	K189T	Q107L and/or K1193T variant	no
46	GGTGCCTATTTAGTTGAGGAGTTACCACC	**1**	0	**22**	**1**	**3**	0	0	0	single_mutant	single_mutant/*wt*	CVMNT	NGFSDD	V62M	K189T	Q107L and/or K1193T variant	**yes**
158	GGCGXCCGTCCXATCGXCGXATTACTTTC	0	0	**2**	**1**	0	0	0	0	double_mutant/triple_mutant	double_mutant	SVMNT	NDFCDY	V424I/*wt*	K189T	R1133S + E1011K variant	**yes (2)** / no (1)
155	GGCGCCCATCTAATCGCCGGATTACTTTC	0	0	0	**24**	0	**11**	**21**	0	triple_mutant	triple_mutant	SVMNT	NDFCDY	V424I (and 1 *wt*)	K189T/*wt*(1)	R1133S + E1011K variant	**yes (51)**/no(4)
29	NNCGCCCATCTAATCGCCGGATTACTTTC	0	0	0	**11**	0	0	0	0	triple_mutant	triple_mutant	SVMNT	NDFCDY	V424I	K189T/*wt*(1)	R1133S + E1011K variant	no
95	GGCGCCNATCTAATCGCCGGATTACTTTC	0	0	0	**3**	0	0	0	0	triple_mutant	triple_mutant	SVMNT	NDFCDY	V424I	K189T		**yes**

14	AACGTCCGTCCAATCGC GGGATTACTTCC	0	0	0	**16**	**2**	0	**2**	0	triple_mutant	triple_mutant	SVMNT	NDFCDY	*wt*	*wt*/K189T(2)	R1133S + E1011K variant	no
130	GACGTCCATCCAATCGC GGGATTACTTTC	0	0	0	**2**	0	0	0	**1**	triple_mutant	triple_mutant	SVMNT	NDFCDY	V424I/ *wt*	K189T/*wt*	R1133S + E1011K variant	no (2)/**yes (1)**
7	AACGTCCATCTAATCGC GGGATTACTTTC	0	0	0	**1**	0	0	**2**	0	triple_mutant	triple_mutant	SVMNT	NDFCDY	V424I	*wt*/G449C	R1133S + E1011K variant	no
57	GGNGCCNATTTAATTGC GGAGTTACCACC	0	0	0	0	**1**	0	0	0		single_mutant	CVMNT/ SVMNT	NGFSDD	V62M	K189T	mixed	**yes**
132	GAXXXCCATCTXATCGCX GGATTACTTTC	0	0	0	**1**	0	0	0	0	triple_mutant	triple_mutant	SVMNT	NDFCDY	V424I	K189T		no
149	GGCGCCCGTCCAATTGC GGAGTTACCACC	0	0	0	0	0	0	0	**3**	triple_mutant	*wt*	SVMNT	NDFCDY	*wt*	K189T	Q107L and/or K1193T variant	no
109	GGCGCCCGTCTAATTGA GGGATTACTTTC	0	0	0	0	0	0	**2**	0	triple_mutant	triple_mutant	SVMNT	NDFCDY	*wt*	K189T(1)/*wt*(1)	R1133S + E1011K variant	no
24	AXXXXCCNXCCXATCNXX GGATTACTTCC	0	0	0	0	0	**1**	0	0	triple_mutant	incomplete_mut	SVMNT	NDFCDY	V424I	*wt* incomplete	R1133S + E1011K variant	no
58	GGCGTCCATTTAATTGCC GGATTACTATC	0	0	0	0	0	0	0	**1**	triple_mutant	triple_mutant	SVMNT	NDFCDY	*wt*	K189T	R1133S + E1011K variant	no
59	GGCGNCCNTCTAATXGC NGGATTACTTNC	0	0	0	0	0	0	**1**	0	triple_mutant	triple_mutant	SVMNT	NDFCDY	V424I	K189T	R1133S + E1011K variant	no

1050 **Table 3. Haplotype frequencies in ART and partner drug resistance associated genes.**

			2003-2005		2008-2012		2014-2018		X^2 p-value
			n/n_{tot}	% (95%CI)	n/n_{tot}	% (95%CI)	n/n_{tot}	% (95%CI)	
ART	*K13*	G449C*	1/141	0.7% (0.1-4.9)	0/68	0%	1/45	2.2% (0.3-73.4)	0.03621
		K189T	94/141	66.7% (58.4-74.0)	42/68	61.8% (49.6-73.6)	25/45	55.6% (40.7-73.4)	
		wt	15/141	10.6% (6.5-17.0)	16/68	23.5% (14.9-73.6)	3/45	6.7% (2.1-73.4)	
		wt incomplete	29/141	20.6% (14.6-28.1)	10/68	14.7% (8.0-73.6)	14/45	31.1% (19.2-73.4)	
		missing	2/141	1.4% (0.4-5.6)	0/68	0%	2/45	4.4% (1.1-73.4)	
	ubp1	Q107L and/or K1193T type	60/141	42.6% (34.6-50.9)	6/68	8.8% (4.0-18.4)	3/45	6.7% (2.1-19.0)	< 2.2e-16
		R1133S type	21/141	14.9% (9.9-21.8)	7/68	10.3% (4.9-20.2)	1/45	2.2% (0.3-14.6)	
		R1133S + E1011K type	33/141	23.4% (17.1-31.2)	53/68	77.9% (66.4-86.3)	41/45	91.1% (78.3-96.7)	
		mixed Q107L/K1193T+ R1133S	3/141	2.1% (0.7-6.4)	1/68	1.5% (0.2-9.9)	0/45	0	
		wt or *wt* incomplete	24/141	17.0% (11.6-24.2)	1/68	1.5% (0.2-9.9)	0/45	0	
	coronin	V424I	78/141	55.3% (47.0-63.4)	41/68	60.3% (48.2-71.3)	37/45	82.2% (68.0-91.0)	0.002743
		V62M	29/141	20.6% (14.6-28.1)	5/68	7.4% (3.1-16.6)	0/45	0%	
		wt	30/141	21.3% (15.3-28.9)	20/68	29.4% (19.7-41.4)	8/45	17.8% (9.0-32.0)	
		mixed	0/141	0%	1/68	1.5% (0.2-9.9)	0/45	0%	
		incomplete	4/141	2.8% (1.1-7.4)	1/68	1.5% (0.2-9.9)	0/45	0%	
SP	*dhfr*	single mutant (S108N)	98/141	69.5% (61.4-76.6)	6/68	8.8% (4.0-18.4)	0/45	0%	< 2.2e-16
		double mutant + BR + I164L	32/141	22.7% (16.5-30.4)	0/68	0%	0/45	0%	
		triple mutant	0/141	0%	61/68	89.7% (79.8-95.1)	44/45	97.8% (85.4-99.7)	
		incomplete	3/141	2.1% (0.7-6.4)	0/68	0%	1/45	2.2% (0.3-14.6)	
		missing	6/141	4.3% (1.9-9.2)	1/68	1.5% (0.2-9.9)	0/45	0%	
	dhps	Single mutant K540K	16/141	11.3% (7.0-17.8)	0/68	0%	0/45	0%	< 2.2e-16
		Single mutant A437G	3/141	2.1% (0.7-6.4)	1/68	1.5% (0.2-9.9)	0/45	0%	
		Double mutant	14/141	9.9% (5.9-16.1)	0/68	0%	0/45	0%	
		triple mutant	2/141	1.4% (0.4-5.6)	48/68	70.6% (58.6-80.3)	30/45	66.7% (51.6-79.0)	
		incomplete mutant	7/141	5.0% (2.4-10.1)	13/68	19.1% (11.4-30.4)	12/45	26.7% (15.7-41.6)	
		wt	80/141	56.7% (48.4-64.7)	4/68	5.9% (2.2-14.8)	2/45	4.4% (1.1-16.4)	
		wt incomplete	19/141	13.5% (8.7-20.2)	2/68	2.9% (0.7-11.2)	1/45	2.2% (0.3-14.6)	
CQ and MQ	*crt* (positions 72-76)	CVMNT	65/141	46.1% (38.0-54.4)	2/68	2.9% (0.7-11.2)	0/45	0%	8.37E-16
		SVMNT	49/141	34.8% (27.3-43.0)	60/68	88.2% (78.0-94.1)	32/45	71.1% (56.1-82.6)	
		CVMNT/SVMNT mixed	0/141	0%	1/68	1.5% (0.2-9.9)	0/45	0%	
		incomplete	27/141	19.1% (13.4-26.6)	5/68	7.4% (3.1-16.6)	13/45	28.9% (17.4-43.9)	
	mdr1 (positions 86, 144, 184, 1034,1042, 1246)	NDFCDD	61/141	43.3% (35.3-51.6)	1/68	1.5% (0.2-9.9)	0/45	0%	< 2.2e-16
		ND_CDD	2/141	1.4% (0.4-5.6)	0/68	0%	0/45	0%	
		NDFCDY	17/141	12.1% (7.6-18.6)	60/68	88.2% (78.0-94.1)	42/45	93.3% (81.0-97.9)	
		NGFSDD	43/141	30.5% (23.4-38.6)	5/68	7.4% (3.1-16.6)	0/45	0%	
		NG_SDD	4/141	2.8% (1.1-7.4)	0/68	0%	0/45	0%	
		NDFSDD	1/141	0.7% (0.1-4.9)	0/68	0%	0/45	0%	
		mixed	5/141	3.5% (1.5-8.3)	0/68	0%	0/45	0%	
		incomplete	8/141	5.7% (2.8-11.0)	2/68	2.9% (0.7-11.2)	3/45	6.7% (2.1-19.0)	

*1/2 G449C also accompanied with K189T; both cases mixed inf.
dhps double mutant (A437G
+A581G)
dhps triple mutant (A437G +A581G + K540E)
wt = wilde type
note: The *ubp1*-haplotype with R1133S and E1011K was frequently observed with additional SNP mutations (K764N, K774N, D777G) and a large insert (EQKY) between amino acid positions 2826/2827.

Figure legends

Figure 1 – Annual *P. falciparum* cases in Peru (black line) from 1992-2020, with first-line treatment policy changes (source of data: Centro Nacional de Epidemiología, Prevención y Control de Enfermedades (2020) Sistema de Atención de Solicitudes de Acceso a la Información Pública Vía internet del Ministerio de Salud. Available at: http://www.minsa.gob.pe/portada/transparencia/solicitud/). Artemisinin combination therapies were first introduced in the Amazon region in Peru in 2001, contributing to a dramatic decline in cases. Artesunate mefloquine with primaquine (AS + MQ +PQ) has always been the recommended first-line treatment in the Amazon region (51) with continued high efficacy (57), and AS+SP was used on the North Coast. In 2015, AS+MQ+PQ became the recommended first-line treatment in the whole country (58). Peru reduced malaria case incidence by ≥40% by 2010 using passive case detection (PCD), diagnosis with light microscopy and treatment with AS+MQ as main components of the control program (59). In 2015, with the realization that PCD missed asymptomatic infections (60), focal screening and treatment was introduced, resulting in a further reduction of malaria incidence (50). CQ + PQ = chloroquine + primaquine; SP = sulfadoxine-pyrimethamine; QN = quinine.

Figure 2 – Map of study sites of retrospective sample collection from the Peruvian Amazon region Loreto (grey). The majority of samples were collected in Maynas Province (areas 1, 2, and 3): samples collected in/near the San Juan Bautista district (area 3), which covers part of the urban area of Loreto's capital Iquitos and peri-urban communities south of Iquitos (n=226), and samples from the Mazán district (area 1; n =17) and Punchana district (area 2; n =64) with remote communities living near forest rivers such as the Amazon River and Napo River, North of Iquitos. A final collection of samples from 2018 was available from the Northern Amazon region in Datem del Marañón Province, Pastaza District (area 4, n=5). *P. falciparum* positive samples from previous studies were selected based on geographical representation and parasite density (≥100 p/µl by PCR; geometric mean density 4300±3.1 p/µl).

Figure 3 - Population genetic statistics. A) Genetic diversity (expected heterozygosity, *He*) for each barcode locus (black dots) grouped by time-period. Boxplots show a decrease in the median [interquartile range] of *He* after the first time period (2003-2005). Since differences in He might be due to unequal sampling in districts through time, we assessed He within San Juan Bautista district that was sampled at all three time-periods. This confirmed decreasing diversity over time, with a pronounced decrease in He in 2014-2018 ($p > 0.001$, Figure S5 and table S10). **B)** Genetic differentiation between the three populations measured as F_{ST} (Weir & Cockerham, 1984) using the R package diveRsity. Number of individuals for each population: $n_{2003\text{-}2005} = 118$; $n_{2008\text{-}2012} = 65$; $n_{2014\text{-}2018} = 38$. In Figure S5 *He* by time and district is plotted and in Figure S6 the differentiation measures $G`_{ST}$ (Hedrick, 2005) and Jost's D (Jost 2008) are plotted.

Figure 4 - Dynamics of 28-SNP barcode multilocus lineages. Area plot showing the proportions of each ML-lineage detected in the three different time periods in study samples (n=254) from Peru. ML-lineages were identified, clustered using genetic distance between barcodes with the poppr package in R, and given an identifying number. ML-lineages differed by multiple SNPs (≥4 SNPs), enabling lineage classification even when barcodes had some missing or heterozygous genotypes. Lineages are characterized by unique barcodes and resistance genotypes and listed in table 2.

Figure 5 - Discriminant analysis of principal components (DAPC). Scatter plot of discriminant analysis (DA) eigenvalues 1 and 2 using all biallelic SNPs in the core targeted region (excl. amplicons targeting repetitive regions and non-nuclear targets), showing a differentiation between Peruvian *P. falciparum* samples collected before 2008 and those afterwards (x-axis, PC1), and a subsequent separation along the y-axis (PC2) from 2014

1094 to more recent years and along geographic distance. SNPs contributing most to the DAPC are listed in Table
1095 S13. DAPC was performed with 40 principal components and 7 discriminants as determined through cross-
1096 validation. The increased resolution in the DAPC allowed the detection of greater genetic variation in isolates
1097 from 2014-2018 (black shapes), compared to lineage analysis.

1098 **List of supplementary material:**

1099 **Supplementary files**

1100 **Supplementary file 1: Variants of interest for drug resistance (.csv)**

1101 **Supplementary file 2: PF AmpliSeq design: primer sequences and locations on the genome (.xlsx)**

1102 **Supplementary file 3: Supplementary methods (.docx)**

1103 **Supplementary file 4: Pairwise linkage disequilibrium (rbarD) and allele loadings for within-country SNP**
1104 **selection for *P. falciparum* Ampliseq Peru (.xlsx)**

1105

1106 **Supplementary figures and tables**

1107 **Figure S1. Distribution of depth of coverage of aligned high quality reads past filter (format field DP) per**
1108 **amplicon region.**

1109 **Table S1. Amplicons with low genotype depth.**

1110 **Table S2. Amplicons with high genotype depth of coverage (>150).**

1111 **Table S3. Amplicons in conserved regions.**

1112 **Figure S2. Effect of selective whole genome amplification (sWGA)**

1113 **Table S4. Error rates in 3D7 replicates without and with sWGA in different subsets of loci.**

1114 **Table S5. Genotyping known variants in previously genotyped controls**

1115 **Table S6. Detection limit of variant loci in 3D7-Dd2 mock samples**

1116 **Table S7. Complexity of infection analyses.**

1117 **Figure S3. Proportion multiple clone infections in Peru.**

1118 **Table S8. Pairwise comparison of *hrp2/hrp3* classification by PCR and Pf AmpliSeq**

1119 **Table S9 Barcode SNPs.**

1120 **Figure S4. Principal component analysis of samples (n=254) collected in Peru between 2003 and 2018.**

1121 **Figure S5. Expected Heterozygosity by time period and district.**

1122 **Table S10. p-values for pairwise comparisons of *He*.**

1123 **Figure S6. Genetic differentiation between parasite populations in the three time periods**

1124 **Figure S7. Minimum spanning network (nLV graph) of multilocus lineages**

1125 **Table S11. Linkage disequilibrium**

1126 **Table S12. 28-SNP barcode loci that become fixed over time**

1127 **Table S13 Contributions of alleles to DAPC.**

1128 **Figure S8. Copy number variations in A) plasmepsin II gene (pm2) and B) multidrug resistance gene 1 (mdr1)**

1129 **Table S14 Cost comparison AmpliSeq vs WGS**

1130 **Table S15: Laboratory strains included in assay validation**

1131 **Figure S9. Distributions of log mean depth ratio's for all samples for each *hrp3* amplicon and *hrp2* amplicon**

1132 **Table S16. Cutoff thresholds for *hrp2* and *hrp3* determination of deletions for each amplicon.**

1133